© 2014. Published by The Company of Biologists Ltd | Journal of Cell Science (2014) 127, 2005–2016 doi:10.1242/jcs.142174

RESEARCH ARTICLE

The Tea4–PP1 landmark promotes local growth by dual Cdc42 GEF recruitment and GAP exclusion

Kyriakos Kokkoris, Daniela Gallo Castro and Sophie G. Martin*

ABSTRACT

Cell polarization relies on small GTPases, such as Cdc42, which can break symmetry through self-organizing principles, and landmarks that define the axis of polarity. In fission yeast, microtubules deliver the Tea1–Tea4 complex to mark cell poles for growth, but how this complex activates Cdc42 is unknown. Here, we show that ectopic targeting of Tea4 to cell sides promotes the local activation of Cdc42 and cell growth. This activity requires that Tea4 binds the type I phosphatase (PP1) catalytic subunit Dis2 or Sds21, and ectopic targeting of either catalytic subunit is similarly instructive for growth. The Cdc42 guanine-nucleotide-exchange factor Gef1 and the GTPase-activating protein Rga4 are required for Tea4–PP1-dependent ectopic growth. Gef1 is recruited to ectopic Tea4 and Dis2 locations to promote Cdc42 activation. By contrast, Rga4 is locally excluded by Tea4, and its forced colocalization with Tea4 blocks ectopic growth, indicating that Rga4 must be present, but at sites distinct from Tea4. Thus, a Tea4–PP1 landmark promotes local Cdc42 activation and growth both through Cdc42 GEF recruitment and by creating a local trough in a Cdc42 GAP.

KEY WORDS: Cdc42, *Schizosaccharomyces pombe*, Cell polarization, Type I phosphatase, Tea4, PP1

INTRODUCTION

How cells polarize in response to intracellular or extracellular cues is an important cell biological question. It is well understood that small Rho-family GTPases are at the core of the polarization machinery. In fungal and metazoan systems, the small GTPase Cdc42, which becomes active upon GTP binding, plays a key function in cell polarization (Harris and Tepass, 2010; Bi and Park, 2012; Thompson, 2013). Exchange of GDP for GTP is promoted by guanine-nucleotide-exchange factors (GEFs), whereas GTPase-activating proteins (GAPs) promote GTP hydrolysis. In its active state, Cdc42 then binds effectors to activate signaling pathways, organize the cytoskeleton and promote polarized exocytosis.

Important work using the budding yeast system has shown that Cdc42 is capable of breaking symmetry by spontaneously forming a polarized cluster (Gulli et al., 2000; Irazoqui et al., 2003; Wedlich-Soldner et al., 2003). In mutant *Saccharomyces cerevisiae* cells lacking the landmarks that normally define the site of polarization, the stochastic formation of small Cdc42 clusters is amplified through positive-feedback mechanisms, leading to formation of a single polarization site for bud emergence at a random position (Irazoqui et al., 2003; Wedlich-Soldner et al., 2003; Slaughter et al., 2009; Johnson et al., 2011). One important question is how this self-organizing system is normally harnessed by landmarks to promote Cdc42 activation at specific cortical sites in response to either intracellular or extracellular cues (Bi and Park, 2012). Landmarks might promote Cdc42 activity by locally tipping the balance towards activation, but the specific mechanisms at work are unknown.

Fission yeast (*Schizosaccharomyces pombe*) cells are highly polarized cells that grow by tip extension. Growth is stereotypically regulated during the cell cycle, where newborn cells initially grow in a monopolar manner at the old cell end until they initiate bipolar growth in the G2 phase of the cell cycle, a transition named NETO for 'new end take-off' (Mitchison and Nurse, 1985; Martin and Chang, 2005). As in other organisms, Cdc42 is central for polarized growth. Cdc42 is activated by two GEFs, Scd1 and Gef1, both of which localize to cell poles, and, like Cdc42, are together essential for cell viability (Chang et al., 1994; Miller and Johnson, 1994; Coll et al., 2003; Hirota et al., 2003; Das et al., 2009). Scd1 plays a major role, as *scd1Δ* cells are almost round, exhibiting much wider growth zones than wild-type cells (Chang et al., 1994; Kelly and Nurse, 2011). Gef1 plays a comparatively minor role in defining the size of the growth zone, but its deletion leads to monopolar growth defects (Coll et al., 2003). So far, a single Cdc42 GAP has been described, Rga4, which localizes along the sides of the cell and acts additively to Scd1 to define the width of growth zones (Das et al., 2007; Tatebe et al., 2008; Kelly and Nurse, 2011). *rga4Δ* cells also exhibit monopolar growth defects (Das et al., 2007). One important role of Cdc42 for cell morphogenesis is to promote the polarized exocytosis of cell-wall-remodeling enzymes to drive polar cell growth. For this, Cdc42 is thought to activate both the formin For3, which assembles polarized arrays of actin cables for myosin-V-dependent vesicle delivery, and the exocyst complex, which promotes the tethering of exocytic vesicles at the plasma membrane (Martin et al., 2007; Rincón et al., 2009; Bendezú and Martin,, 2011; Estravís et al., 2011; Nakano et al., 2011; Bendezú et al., 2012).

Whereas Cdc42 is required for polarized growth per se, the location of this process is defined by the Tea1–Tea4 complex, which is delivered at cell poles by the microtubule cytoskeleton (Mata and Nurse, 1997; Martin et al., 2005; Tatebe et al., 2005; Martin, 2009). In this complex, Tea1 links Tea4 to the microtubule end, likely through the CLIP-170 protein Tip1, and to the cell cortex, through the prenylated anchor Mod5 (Snaith and Sawin, 2003; Martin et al., 2005; Tatebe et al., 2005; Bicho et al., 2010). In the absence of *tea1* or *tea4*, cells do not precisely position growth at cell poles, resulting in curved cells and, upon

University of Lausanne, Department of Fundamental Microbiology, Biophore Building, CH-1015 Lausanne, Switzerland.

*Author for correspondence (sophie.martin@unil.ch)

Received 4 September 2013; Accepted 23 January 2014

Journal of Cell Science

Journal of Cell Science (2014) 127, 2005–2016 doi:10.1242/jcs.142174

growth re-initiation, often place growth at a site distinct from cell poles, forming T-shaped cells. The Tea1–Tea4 complex is also essential for initiation of growth at the second cell pole at NETO. Consistently, numerous polarization factors localize at a single cell pole in *tea1Δ* or *tea4Δ* cell, such as active Cdc42 and its activators, the formin For3, the exocyst complex, the actin cytoskeleton and cell wall enzymes (Cortés et al., 2002; Castagnetti et al., 2005; Martin et al., 2005; Tatebe et al., 2005; Snaith et al., 2011; Das et al., 2012).

The Tea1–Tea4 complex is also required to nucleate plasma-membrane-associated gradients of the DYRK-family kinase Pom1 at cell poles (Bähler and Pringle, 1998; Celton-Morizur et al., 2006; Padte et al., 2006; Hachet et al., 2011). Here, Tea4 acts as phosphatase regulatory subunit by recruiting the type I phosphatase (PP1) subunit Dis2 to cell poles to promote local Pom1 de-phosphorylation, revealing a membrane-binding region (Alvarez-Tabarés et al., 2007; Hachet et al., 2011). Tea4 requires both its SH3 domain and an RVxF motif to associate with Dis2 *in vivo*, and also binds Pom1 through its SH3 domain (Alvarez-Tabarés et al., 2007; Hachet et al., 2011). Lateral movement of Pom1 at the plasma membrane and auto-phosphorylation-driven membrane detachment then shape the gradients. Although it has been proposed that Pom1 gradients monitor the cell length for mitotic commitment (Martin and Berthelot-Grosjean, 2009; Moseley et al., 2009; Bhatia et al., 2014), *pom1Δ* cells also display morphological and NETO defects similar to those of *tea1Δ* or *tea4Δ* cells (Bähler and Pringle, 1998; Hachet et al., 2012), indicating it is an important effector of the Tea1–Tea4 complex in cell polarization.

How does the Tea1–Tea4 landmark regulate bipolar antipodal growth? Answering this question has been difficult, in part due to the positive feedbacks that make cell polarization a robust process. Similar to the budding yeast case, positive and negative feedbacks have been proposed to underlie Cdc42 self-organization, leading to oscillations of Cdc42 activity between the two cell poles (Bendezú and Martin, 2012; Das et al., 2012). In addition, microtubule organization and cell shape form a self-reinforcing system, in which the cell shape provides physical constraints that align microtubules along the length of the cell to deliver landmarks to cell extremities, which in turn reinforce the rod shape by marking the cell ends for growth (Terenna et al., 2008; Minc et al., 2009).

Two main hypotheses for the role of the Tea1–Tea4 complex have been put forward. First, we proposed that recruitment of the formin For3 to cell poles might be a crucial step for NETO. In support of this idea, Tea4 binds For3 directly, and artificial targeting of For3 to both cell ends is sufficient to restore bipolar growth in the absence of *tea4* (Martin et al., 2005). However, as *for3Δ* cells are only partly NETO deficient and exhibit complex growth patterns (Feierbach et al., 2004), For3 recruitment might not be the only necessary step for NETO. Second, Tatebe et al. proposed that Pom1 might promote the exclusion of the Cdc42 GAP Rga4 from cell poles to allow bipolar Cdc42 activation, although Rga4 is unlikely to be a Pom1 substrate (Tatebe et al., 2008). In support of this idea, Rga4, normally present at the sides of the cell, covers the entire non-growing cell end in *tea1Δ*, *tea4Δ* and *pom1Δ* cells (Tatebe et al., 2008). However, *rga4* deletion fails to restore bipolar growth to *pom1Δ* cells, suggesting again that absence of Rga4 does not suffice for NETO.

Here, we have tested the function of Tea4 as a landmark protein by using a novel assay for Tea4-mediated cell polarization. By ectopically targeting Tea4 to the sides of the cell, we show that Tea4 is instructive for Cdc42 activation and cell growth. Surprisingly, Tea4-mediated ectopic growth is largely independent of For3 and Pom1. Instead it requires PP1 binding, and the Cdc42 GEF Gef1 and Cdc42 GAP Rga4. We show that Gef1 is recruited and Rga4 locally excluded by Tea4, and that this local exclusion is necessary for polarized growth. Ectopically localized PP1 also promotes growth in a Gef1- and Rga4-dependent manner. These data suggest that the Tea4–PP1 complex might promote local Cdc42 activation and polarized growth by dual recruitment of an activator and exclusion of a negative factor.

RESULTS

Tea4 is instructive for growth

To test whether Tea4 is instructive for growth, we targeted Tea4 ectopically to the sides of fission yeast cells. We constructed a fusion protein between Cdr2, a kinase that localizes throughout interphase to a broad band of nodes at the cell equator (Morrell et al., 2004), and Tea4N (Fig. 1A). The Tea4N allele lacks its C-terminal Tea1-interacting region (Martin et al., 2005), to prevent localization of the Cdr2–Tea4N fusion to cell tips. To visualize the fusion protein, GFP, CFP or mCherry was included between Cdr2 and Tea4N. As predicted, in wild-type cells, the fusion protein localized to the sides of the cell (Fig. 1B). It also localized in the nucleus. In these cells, which express native Tea4, Cdr2–Tea4N had little influence on cell shape, although cells were longer than wild-type cells (data not shown). However, when expressed in *tea4Δ* cells, which lack endogenous cell-tip-localized Tea4, Cdr2–Tea4N localized to a large portion of the cell periphery and promoted a localized widening of the cells (a bulge) at or near the cell equator in >50% of exponentially growing cells (n>300 from three independent experiments; Fig. 1C, see Fig. 3B for quantification). The observation of bulges in *tea4Δ*, but not wild-type cells, suggests that endogenous growth sites compete with establishment of new growth sites, as has been previously proposed (Castagnetti et al., 2007). The extended length of cells expressing the Cdr2–Tea4N fusion might thus also favor the appearance of bulges. We note that this phenotype is distinct from the T-shapes exhibited by *tea4Δ* cells, which occur upon growth re-initiation. By contrast, *tea4Δ* cells expressing only Cdr2, as a control, did not display medial bulges. All further experiments were thus conducted in *tea4Δ* mutant background. These data show that ectopic Tea4 is instructive for growth.

We followed the formation of this bulge in flow-chambers (Fig. 1D; supplementary material Fig. S1, Movie 1). Cells without an apparent bulge formed a bulge *de novo*, which grew by about 2 µm in diameter over 4–6 hours. Once formed, bulges were maintained in the progeny and kept widening in sequential generations (supplementary material Movie 1). Overtime, swollen, pear-shaped and round cells also accumulated. Cells continued dividing even upon steady-state expression of Cdr2–Tea4N, either in liquid culture or in flow-chambers, although 9%±3 (means±s.d.) of cells died immediately after cell division in the latter situation. We also observed that Cdr2–Tea4N was able to partly restore bipolar growth patterns (50%±5 bipolar cells, compared to over 90% monopolar cells for *tea4Δ*), though how this restoration of bipolar growth occurs is currently unclear.

Tea4 recruits active Cdc42 independently of growth

The growth conferred by ectopic Tea4 provided a novel assay to test the genetic requirements for growth at a naïve site, which

Journal of Cell Science (2014) 127, 2005–2016 doi:10.1242/jcs.142174

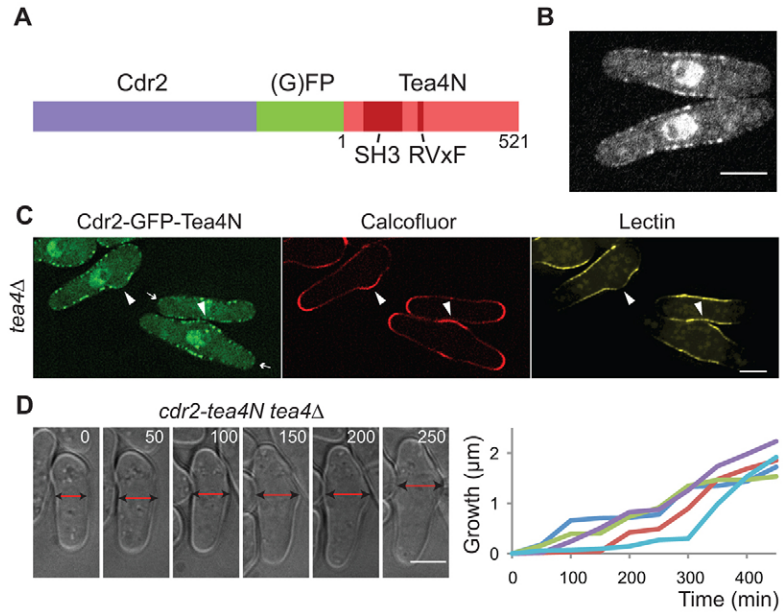

Fig. 1. Tea4 is instructive for growth. (A) Schematic representation of the Cdr2–GFP–Tea4N fusion. (B) Localization of Cdr2–GFP–Tea4N in wild-type cells. (C) Cdr2–GFP–Tea4N expression in *tea4Δ* cells leads to medial bulge formation. Cells stained with TRITC-Lectin, and returned to growth for 1 h, stained with Calcofluor White. Zones of growth are devoid of lectin and stained with Calcofluor White. Arrowheads point to medial growing bulges. Note that Cdr2–GFP–Tea4N, like Cdr2, often becomes displaced from zones of growth (arrowheads). In *tea4Δ* cells, Cdr2–GFP–Tea4N exhibits a more spread localization also to cell tips (arrows) than in wild-type cells (see B). (D) Timelapse images of *tea4Δ cdr2-GFP-tea4N* cells grown in a flow chamber. Time is indicated in minutes. The graph on the right indicates the increase in cell width of five cells over time. Scale bars: 5 μm.

bypasses the difficulties caused by the feedback mechanisms that render polarized growth at cell ends robust.

In cells exhibiting ectopic growth, all the polarity factors that were examined, whose bipolar localization depends on Tea4, localized ectopically to cell sides – i.e. Pom1, Dis2, active Cdc42 (as labeled by a CRIB–GFP reporter), its GEFs Scd1 and Gef1, the formin For3 and the exocyst subunit Exo70, as well as actin structures (Fig. 2A–C; supplementary material Table S2). Microtubules were aberrantly organized, with many microtubules misaligned and pointing into the bulged region (Fig. 2C). This disorganization was probably a consequence of the aberrant cell shape, as it was not observed in rod-shaped cells of the same genotype. In addition, Tea1 was also localized to cell sides (Fig. 2A; supplementary material Table S2), although it does not directly bind the Tea4N allele (Martin et al., 2005), suggesting it might be deposited there by misaligned microtubules. Thus, once ectopic growth has been initiated, all factors examined normally present at cell tips are also recruited to this ectopic growth site.

To distinguish between factors recruited as a consequence of growth from factors recruited more directly by ectopic Tea4, we investigated the localization of these same factors at earlier time points, prior to ectopic growth. In *tea4Δ cdr2-tea4N* cells of normal rod morphology, Tea1 and Scd1 were not enriched on cell sides, suggesting these factors might be recruited as a consequence of cell growth, or present at cell sides below detection levels. Similarly, the actin and microtubule cytoskeleton appeared normal. However, actin cables were likely not correctly oriented, as the type V myosin Myo52, used as marker for the barbed ends of actin filaments, localized to cell sides even in rod-shaped cells (Fig. 2D). Consistently, For3, as well as Pom1 and Dis2, were present at cell sides in rod-shaped cells (Fig. 2E,F; supplementary material Table S2), in agreement with their demonstrated direct binding with Tea4 (Martin et al., 2005; Alvarez-Tabarés et al., 2007; Hachet et al., 2011). Of note, the recruitment of Pom1, which interferes with Cdr2 localization (Martin and Berthelot-Grosjean, 2009; Moseley et al., 2009), likely contributes to the spreading of Cdr2–Tea4N around a large part of the cell periphery. Similarly, Exo70 was also detected on cell sides (Fig. 2E). Importantly, CRIB and Gef1 were also present at the sides of rod-shaped cells expressing ectopic Tea4 [44%±8 and 23%±5 of rod-shaped cells, respectively (means±s.d.); Fig. 2G; supplementary material Table S2]. We note that the Gef1–GFP signal is weak, suggesting our measurements might underestimate the number of cells with this protein on cell side. By contrast, CRIB and Gef1 were absent from the sides of interphase cells, and only localized medially in anaphase, in preparation for cytokinesis (supplementary material Fig. S2). Thus, active Cdc42 and other, but not all, polarity factors are recruited by Tea4 independently of cell growth.

Tea4-dependent ectopic growth does not require Pom1

We tested the genetic requirements for bulge formation. Tea4 contains an RVxF motif, necessary to bind Dis2, and an SH3 domain, essential for binding both Pom1 and Dis2. Consistently, in $tea4^{RVxF*}$ and $tea4^{SH3*}$ mutants, in which the RVxF and SH3 domain, respectively, are mutated at the endogenous locus, Dis2 is absent from cell ends (Alvarez-Tabarés et al., 2007; Hachet et al., 2011), and Pom1 localization is absent from cell ends in $tea4^{SH3*}$ mutants, and strongly reduced in $tea4^{RVxF*}$ mutants (Hachet et al., 2011). The $tea4^{SH3*}$ mutant exhibited a *tea4Δ*-like phenotype with 53%±4 monopolar cells (versus 11%±8 of wild-type and 90%±2 of *tea4Δ* cells) (mean±s.d.), off-centered septa and a large proportion of T-shaped cells in re-feeding experiments (see Fig. 3E). Similar morphological defects were previously described for $tea4^{RVxF*}$ mutant alleles (Alvarez-Tabarés et al., 2007). Cdr2–Tea4N with *RVxF** or *SH3** mutations localized to cell sides, but did not promote ectopic growth in *tea4Δ* cells (Fig. 3A,B). We note that, for unknown reasons, the Cdr2–$Tea4N^{SH3*}$ fusion was expressed at lower levels and was not present in the nucleus. This suggests Dis2 and/or Pom1 might be crucial for the initiation of ectopic growth.

Surprisingly, deletion of *pom1* reduced, but did not abrogate bulge formation in *tea4Δ cdr2-tea4N* cells (Fig. 3C). We note though that *pom1* deletion prevented cell lengthening, in agreement with previous work showing that ectopic Pom1 recruitment to cell sides delays mitotic commitment (Martin and Berthelot-Grosjean, 2009; Moseley et al., 2009; Hachet et al., 2011). This reduction in length might contribute to the reduced

Journal of Cell Science (2014) 127, 2005–2016 doi:10.1242/jcs.142174

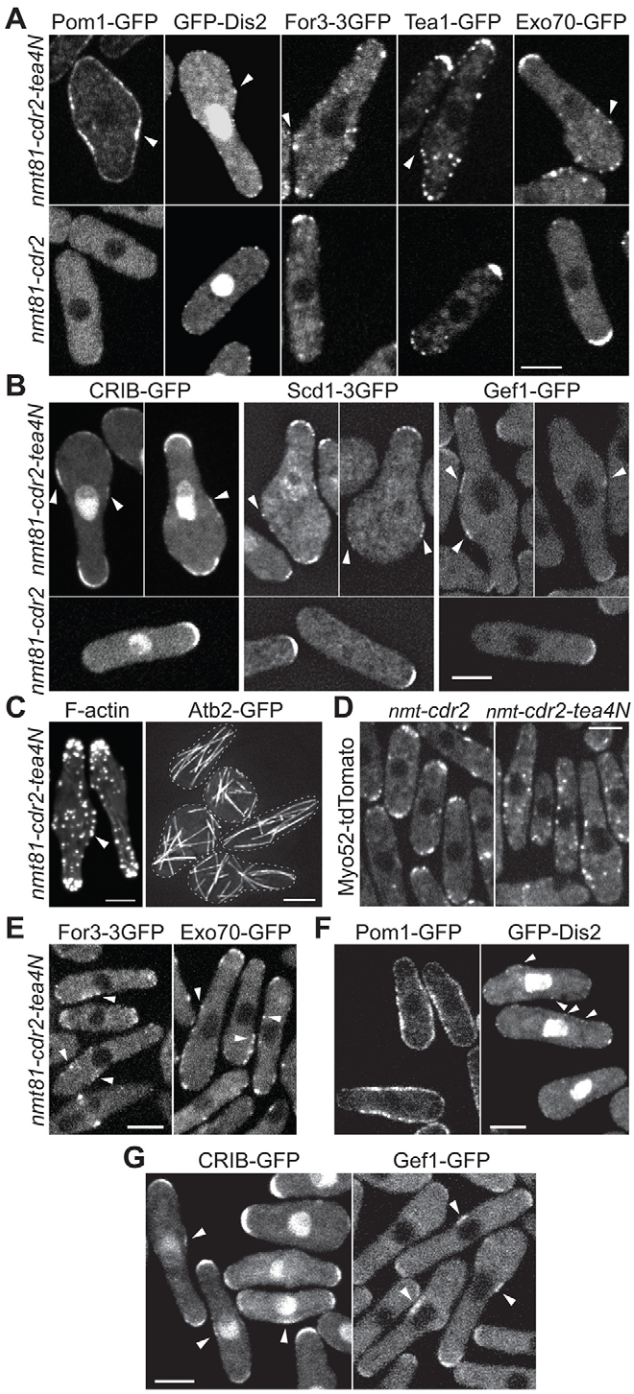

Fig. 2. Localization of polarity factors to sites of ectopic Tea4 localization. (A) Localization of Pom1–GFP, GFP–Dis2, For3–3GFP, Tea1–GFP and Exo70–GFP in *tea4Δ cdr2-tea4N* bulged cells (top). *tea4Δ* cells expressing a transgene lacking the *tea4N* moiety are used as a control (bottom). (B) Localization of active Cdc42, as labeled by CRIB–GFP, as well as the Cdc42 GEFs Scd1–3GFP and Gef1–GFP in *tea4Δ cdr2-tea4N* bulged cells. *tea4Δ* cells expressing a transgene lacking the *tea4N* moiety are used as a control (bottom). (C) Actin organization as labeled by phalloidin staining (left) and microtubule organization as labeled by Atb2–GFP (right), in *tea4Δ cdr2-tea4N* bulged and rod-shaped cells. Maximum projection of spinning disk confocal sections are shown. (D) Localization of Myo52-tdTomato in rod-shaped and bulged *tea4Δ cdr2-tea4N* cells (right). *tea4Δ* cells expressing a transgene lacking the *tea4N* moiety are used as a control (left). (E) For3–3GFP and Exo70–GFP are recruited to cell sides independently of cell shape in *tea4Δ cdr2-tea4N* cells. (F) Pom1–GFP and GFP–Dis2 are recruited to cell sides independently of cell shape in *tea4Δ cdr2-tea4N* cells. (G) Active Cdc42, as labeled by CRIB–GFP, and Gef1–GFP are recruited to cell sides (arrowheads) independently of cell shape in *tea4Δ cdr2-tea4N* cells. Cdr2–Tea4N was induced for >28 h in A–C and 18–20 h in D–G. Scale bars: 5 μm.

occurrence of bulged cells, as new growth sites can form only at a distance from pre-existing ones (Castagnetti et al., 2007). This result prompted us to test whether Pom1 was able to promote ectopic growth: we used Pom1–Cdr2–GFP and Pom1–Cdr2C–GFP (lacking the Cdr2 kinase domain) fusion proteins expressed from the endogenous *pom1* locus, which direct Pom1 to the cell sides (Martin and Berthelot-Grosjean, 2009). In *tea4Δ* cells, which lack the signals necessary for Pom1 localization at cell poles, Pom1–Cdr2 localizes to the cell sides as well as in the cytosol (Fig. 3D). In contrast to Cdr2–Tea4N, however, Pom1–Cdr2 did not promote ectopic growth at cell sides (Fig. 3C). Similar results were observed with a Pom1–Mid1C fusion that also targets Pom1 all around the cell periphery in both wild-type and *tea4Δ* cells (Moseley et al., 2009) (Fig. 3C,D). These data suggest that, in contrast to Tea4, Pom1 is not instructive, but is a permissive factor for growth.

We extended these observations to the normal function of Tea4 and Pom1 at cell tips and tested whether Pom1 was sufficient for cell polarization in absence of functional Tea4. For this, we used Pom1^{6A}, an active allele that localizes to the plasma membrane independently of Tea4 (Hachet et al., 2011): In *pom1^{6A}*, mutation of several auto-phosphorylation sites prevents release of Pom1^{6A} from the plasma membrane, leading to its spreading around the cell periphery, which delays cell division (Hachet et al., 2011). *pom1^{6A}* mutant cells had a normal rod-shape, with only 19%±4 monopolar cells (means±s.d.), a centered septum position and with few T-shaped cells in re-feeding experiments (Fig. 3E). Thus, a strong enrichment of Pom1 at cell poles is not necessary for its function in cell morphogenesis. We then combined the *tea4^{SH3*}* and *pom1^{6A}* alleles: Pom1^{6A}–GFP localized to the plasma membrane independently of Tea4 but was unable to restore bipolarity or the rod shape to *tea4^{SH3*}* mutants in re-feeding experiments (Fig. 3E,F). However, it improved septum placement, likely due to the lengthening of the cells. Thus, retargeting of Pom1 to the plasma membrane is not sufficient to rescue the *tea4^{SH3*}* mutant phenotype. Taken together, these results indicate that Pom1 is not the sole target of the Tea4–Dis2 phosphatase and that Dis2 might be a key Tea4 partner for cell polarization.

PP1 is sufficient to induce growth at cell sides

Fission yeast cell express two PP1 catalytic subunits, Dis2 and Sds21. These two proteins are redundant for viability and likely for cell polarization. Indeed, Sds21 occupies the Dis2 location at cell tips when *dis2* is deleted, single deletions have no effect on cell shape, and the double mutant is lethal (Ohkura et al., 1989; Alvarez-Tabarés et al., 2007).

To directly test the possible role of Dis2 in promoting polarized growth, we constructed a Cdr2–Dis2 fusion protein and expressed it in *tea4Δ* cells to promote Dis2 lateral localization in the absence of tip localization. Remarkably, ectopic Dis2 promoted growth very efficiently, with nearly 90% of *tea4Δ* cells exhibiting swelling at the cell middle, becoming round or pear shaped (Fig. 4A,C). This effect required Dis2 activity, as a predicted phosphatase-dead Dis2 mutant (Cdr2–Dis2^{H247K}) did not promote

Journal of Cell Science (2014) 127, 2005–2016 doi:10.1242/jcs.142174

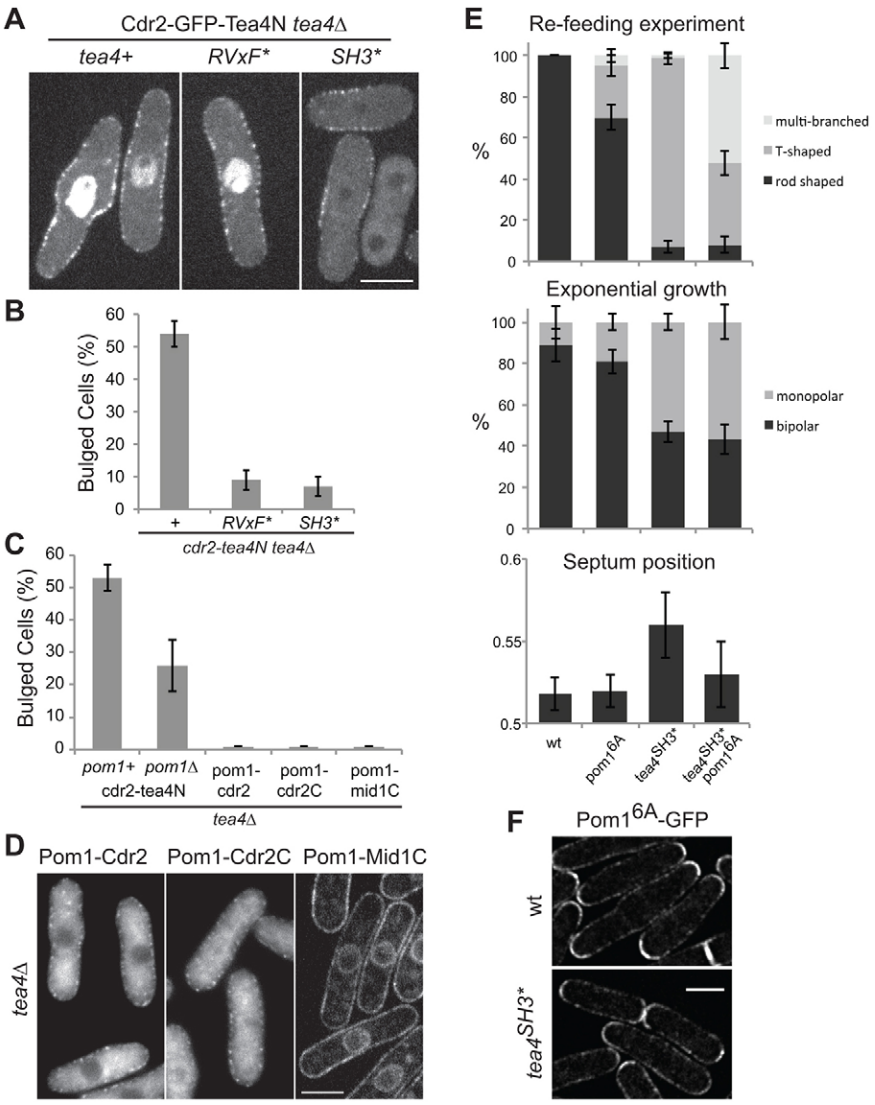

Fig. 3. Tea4-mediated ectopic growth is independent of *pom1*. (A) Localization of Cdr2–GFP–Tea4N, Cdr2–GFP–Tea4N^{RVxF*} and Cdr2–GFP–Tea4N^{SH3*} in *tea4Δ* cells. Maximum projections of three medial spinning disk confocal sections are shown. (B) Tea4 RVxF motif and SH3 domain are required for bulge formation. + indicates wild-type Tea4N moiety. (C) Deletion of *pom1* reduces the occurrence of bulged cells, but ectopically localized Pom1 does not promote ectopic growth. (D) Localization of Pom1–Cdr2–GFP, Pom1–Cdr2C–GFP and Pom1–Mid1–mCherry fusion proteins in *tea4Δ* cells. GFP images are single section epifluorescence images, the mCherry image is a single section spinning disk confocal image. (E) Quantification of cell shape in re-feeding experiments, mono- and bipolarity in exponentially growing septated cells and septum position in wild-type (wt), *pom1^{6A}*, *tea4^{SH3*}* and double mutant cells. (F) Localization of Pom1^{6A}–GFP in wild-type and *tea4^{SH3*}* cells. Results in B, C and E are means±s.d. Scale bars: 5 μm.

bulge formation. Ectopic Dis2 efficiently recruited Pom1, even in absence of Tea4, indicating that the main role for Tea4 in Dis2 phosphatase regulation is as a targeting device for Dis2 (Fig. 4D). Pom1 recruitment required Dis2 activity, although minor amounts of Pom1 could be detected at the membrane in *tea4Δ cdr2-dis2^{H247K}* cells, suggesting either the H247K mutation does not completely block Dis2 activity, or small amounts of Pom1 are recruited independently of Dis2 activity. Again, Pom1 was not essential for bulge formation (Fig. 4C). Thus, ectopic Dis2 behaved similarly to ectopic Tea4, indicating that this type I phosphatase is a key growth-instructive target of Tea4.

As mentioned above, the PP1 Sds1 might function redundantly with Dis2. Interestingly, in a tandem affinity purification (TAP) of Tea4 complexes, we identified not only Dis2 but also Sds21 (supplementary material Table S3). Furthermore, Tea4–PP1 interaction required a functional Tea4 SH3 domain, as neither Dis2 nor Sds21 were identified in a Tea4^{SH3*}-TAP purification (supplementary material Table S3). We tested the possible role of Sds21 in cell polarization by constructing a Cdr2–Sds21 fusion protein and expressing it in *tea4Δ* cells to promote lateral localization of Sds21. Remarkably, this fusion protein potently promoted medial bulge formation (Fig. 4B,C). Thus, in agreement with the ability of Sds21 to occupy the location of Dis2 in its absence (Alvarez-Tabarés et al., 2007), these data indicate that the two catalytic subunits are largely interchangeable and likely able to dephosphorylate the same substrate(s) for cell polarization.

Tea4 recruits Gef1 to promote ectopic growth

What target(s) might the Tea4–PP1 phosphatase complex regulate? We tested the requirement of other polarity factors for Tea4-mediated ectopic growth. Neither *tea1* nor *exo70* were required for bulge formation (Fig. 5A). Expression of ectopic Tea4 in *tea4Δ for3Δ* cells resulted in micro-colonies. Surprisingly, however, many cells in these colonies exhibited a bulge, indicating that For3 is also not required for this ectopic growth (Fig. 5B). By contrast, deletion of the Cdc42 GEF Gef1 or the Cdc42 GAP Rga4 dramatically lowered Tea4-dependent ectopic growth (Fig. 5A). Tea4-mediated ectopic growth was completely blocked in *rga4Δ gef1Δ* double mutants, suggesting the lack of ectopic growth was not simply due to a global unbalance in Cdc42 activation. We were unable to test the requirement for *scd1*, as *scd1Δ* cells are almost round (Chang et al., 1994). Thus, Tea4 might promote Cdc42 activation by controlling its regulators, possibly through the localized dephosphorylation activity of Dis2.

Journal of Cell Science (2014) 127, 2005–2016 doi:10.1242/jcs.142174

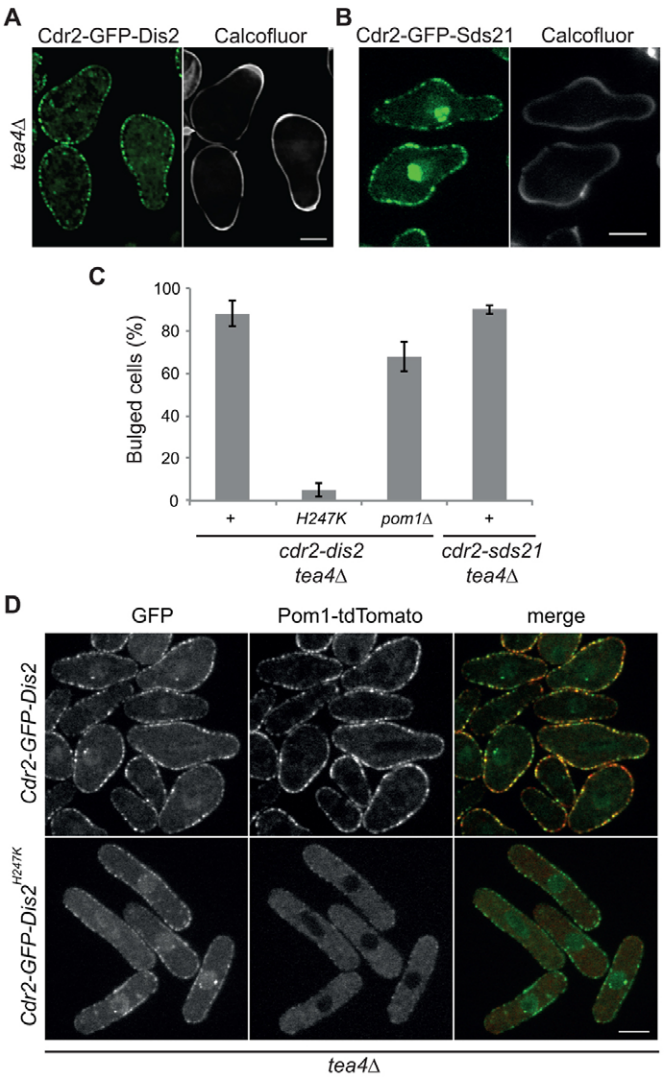

Fig. 4. Ectopic PP1 localization is sufficient to promote growth. (A) Localization of Cdr2–GFP–Dis2 in *tea4Δ* cells and Calcofluor White staining to show bulging cell shape. (B) Localization of Cdr2–GFP–Sds21 in *tea4Δ* cells and Calcofluor White staining to show bulging cell shape. (C) Cdr2–GFP–Dis2 promotes bulge formation, which depends on its activity, but not on *pom1*. Cdr2-GFP-Sds21 also promotes bulge formation. + indicates the wild-type PP1 moiety in the *pom1+* background. All strains are *tea4Δ*. Results are means±s.d. (D) Cdr2–GFP–Dis2 promotes Pom1 cortical localization. Localization of Cdr2–GFP–Dis2 and Pom1–tdTomato in *tea4Δ* cells. Inactive Cdr2–GFP–Dis2^{H247K} localizes to the cell cortex but recruits only minor Pom1 amounts to the plasma membrane. Scale bars: 5 μm.

We investigated whether ectopic Tea4 was able to activate Cdc42 on the sides of *gef1Δ* and *rga4Δ* mutants by investigating CRIB–GFP localization in rod-shaped cells expressing *cdr2-tea4N*. CRIB was absent from the sides of *gef1Δ cdr2-tea4N* cells, but it was still present at the sides of a large proportion of (rod-shaped) *rga4Δ cdr2-tea4N* cells (Fig. 5C; supplementary material Table S2). We note that these *rga4Δ* cells were wider than *rga4*$^{+}$ cells, as previously reported (Das et al., 2007). Thus Rga4 is not required for Tea4-dependent Cdc42 activation at cell sides, but is necessary for bulge formation. By contrast, Gef1 is required for Cdc42 activation at sites of ectopic Tea4 location.

We showed above that ectopic Tea4 recruits Gef1 to cell sides (see Fig. 2G). This recruitment occurred independently of Pom1, as Gef1 was also present on cell sides in *pom1Δ tea4Δ* cells expressing *cdr2-tea4N* (25±3.5% of cells; n>300). Remarkably, Gef1 was also recruited to cell sides in cells expressing the Cdr2–Dis2 fusion prior to bulge formation and was required for Dis2-mediated ectopic growth (Fig. 5D,E). In summary, these data suggest that the Tea4–Dis2 phosphatase recruits Gef1 to mediate Cdc42 activation.

Tea4 binds Rga4 and negatively regulates its localization

In the TAP purification of Tea4 and Tea4^{SH3*} complexes, we identified Rga4 (data not shown). We confirmed this interaction by co-immunoprecipitating Rga4–GFP with Tea4-TAP (Fig. 5F). This interaction was not dependent on Pom1, which has been previously shown to associate with Rga4 (Tatebe et al., 2008). The Tea4^{SH3*}-TAP mutant also co-precipitated Rga4, although somewhat less efficiently, indicating that the interaction was independent of the ability of Tea4 to bind Pom1 or Dis2. Thus, Rga4 associates with Tea4.

Rga4 normally localizes to cell sides and is excluded from cell tips (Das et al., 2007; Tatebe et al., 2008). Upon ectopic Tea4 localization at cell sides, Rga4 remained at cell sides, but appeared less continuous, with clusters of Rga4 present at sites largely distinct from the locations of Cdr2–Tea4N nodes (see Fig. 6B). This is consistent with the observation that Rga4 is largely absent from growing cell tips, where endogenous Tea4 localizes and might exclude Rga4 (Tatebe et al., 2008). However, as Rga4 also did not colocalize strongly with Cdr2 in wild-type or *tea4Δ* cells (data not shown), we could not use this set up to test whether Tea4 promotes Rga4 exclusion. To test this hypothesis, we examined the relative localization of Rga4 with a previously described fusion of Tea4 with the spindle pole body component Ppc89. Ppc89 does not normally localize at the plasma membrane, but for unknown reasons, the Ppc89–Tea4 fusion forms occasional dots located along the cell cortex (Hachet et al., 2011). In these cells, Ppc89–GFP–Tea4 dots at the lateral cortex correlated with a local reduction in Rga4 levels, relative to adjacent regions (Fig. 6A). Similar, although less significant, local reduction was also observed in *pom1Δ* cells. Thus, these data are consistent with the idea that Tea4 promotes local exclusion of Rga4 in a manner that is at least in part *pom1* independent.

Rga4 local exclusion is required for bulge formation

To test whether Rga4 needed to localize at sites distinct from Tea4 for bulge formation, we used an allele of Rga4 previously developed by Kelly and Nurse (cytoRga4–Blt1), which targets a cytosolic form of Rga4 lacking its natural membrane-binding region to the cell cortex through fusion to Blt1 (Kelly and Nurse, 2011). This allele encodes a functional GAP, as it is able to restore cell width to *rga4Δ* cells (Kelly and Nurse, 2011). Blt1 is recruited to medial cortical nodes by Cdr2 and strongly colocalizes with Cdr2 (Moseley et al., 2009). This Blt1–cytoRga4 fusion thus forces colocalization of Rga4 with Cdr2–Tea4N (Fig. 6B).

Expression of the Blt1–cytoRga4 fusion in *tea4Δ cdr2-tea4N* cells blocked bulge formation (Fig. 6C), both when expressed as a sole copy, and when expressed in addition to endogenous Rga4, indicating this allele functions in a dominant manner in this assay. By contrast, expression of a cytosolic form of Rga4 was inactive: it did not support bulge formation as a sole copy, similar to *rga4Δ*, but did not prevent bulge formation when expressed in *rga4*$^{+}$ cells. Thus, forced colocalization of Rga4 with Tea4 prevents growth induction.

Journal of Cell Science (2014) 127, 2005–2016 doi:10.1242/jcs.142174

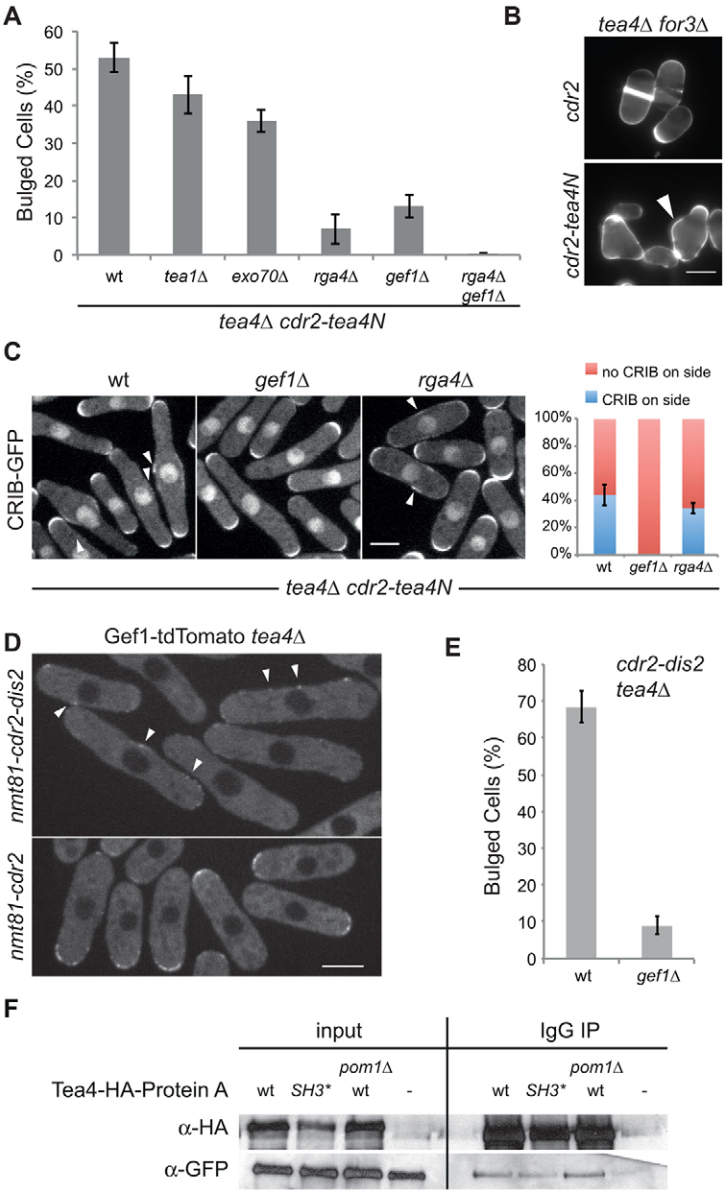

Fig. 5. Gef1 and Rga4 associate with Tea4 and are required for Tea4-mediated ectopic growth. (A) Cdr2–Tea4N-mediated bulge formation in *tea4Δ* cells requires Rga4 and Gef1. wt, wild-type cells. (B) *cdr2-tea4N tea4Δ for3Δ* cells form micro-colonies with cells exhibiting bulges (bottom). *tea4Δ for3Δ* cells expressing a transgene lacking the *tea4N* moiety are used as control (top). (C) Active Cdc42, as labeled with CRIB–GFP, on the sides of *tea4Δ* cells expressing Cdr2–Tea4N, requires Gef1 but not Rga4. Note that *rga4Δ* cells are wider, as previously reported (Das et al., 2007). A quantification is shown on the right. (D) Gef1–tdTomato is recruited to cell sides in *tea4Δ cdr2-dis2* cells (top). *tea4Δ nmt81-cdr2* cells were used as control, where Gef1–tdTomato localizes to one cell pole (bottom). (E) Cdr2–Dis2-mediated bulge formation in *tea4Δ* cells requires Gef1. (F) Rga4-GFP co-immunoprecipitates with Tea4-TAP in wild-type, *pom1Δ* and *tea4*^{SH3*} mutant extracts. Tea4-TAP (HA-TEV–protein-A) was immunoprecipitated (IP) with IgG-loaded beads and detected on blots with an anti-HA antibody. Cdr2–Tea4N was induced for 18–20 h in C and D, and >28 h in A, E and F. Results in A, C and E are means±s.d. Scale bars: 5 μm.

Growth mediated by ectopic Cdr2–Dis2 was similarly dependent on *rga4*: bulge formation required Rga4 and was blocked by forced colocalization of Rga4 with Dis2 (Fig. 5F; Fig. 6D). Thus, Rga4 exclusion by Tea4–PP1 is required for growth to occur. However, as complete removal of Rga4 (in *rga4Δ*) also prevents Tea4–PP1-dependent growth, Rga4 might need to be only locally excluded, but be present in surrounding regions, to promote polarized growth.

DISCUSSION

How cells position their axis of polarity is an important question. Conceptually, this can be thought of as a two-level process: (1) the Cdc42 polarization machinery drives polarization per se through self-organizing feedback mechanisms, and (2) this machinery is harnessed by landmarks at the cell periphery to drive polarization at the appropriate location. In the fission yeast system, which grows by polar extension at both cell poles, the Tea1–Tea4 complex has long been thought to serve as a landmark, because these proteins localize to cell poles and are required to polarize growth at these locations. We show here that Tea4 is also sufficient, when placed at an ectopic location, to promote the local activation of Cdc42 and polarized growth, thereby demonstrating that Tea4 fulfills a true landmark function, marking a site and recruiting the growth machinery. This function is entirely dependent on its association with PP1, which is also sufficient to promote ectopic growth. The Cdc42 GEF Gef1 is necessary for ectopic Cdc42 activation and for local ectopic growth, which further requires the Cdc42 GAP Rga4. We show that Gef1 is recruited by Tea4–PP1. Remarkably, whereas Rga4 is globally necessary, it is locally excluded by Tea4 and needs to be located at a site distinct from Tea4 to allow ectopic growth. This suggests Tea4–PP1 promotes local Cdc42 activation and growth by recruiting a Cdc42 GEF and creating a local decrease in the distribution of a Cdc42 GAP (Fig. 7).

Tea4–PP1 is a landmark for cell polarization

In fission yeast cells, microtubules define the sites of growth. Pharmaceutical or mutational alterations of microtubules modify growth patterns (Umesono et al., 1983; Sawin and Snaith, 2004). Importantly, two recent studies have shown, through physical

Journal of Cell Science (2014) 127, 2005–2016 doi:10.1242/jcs.142174

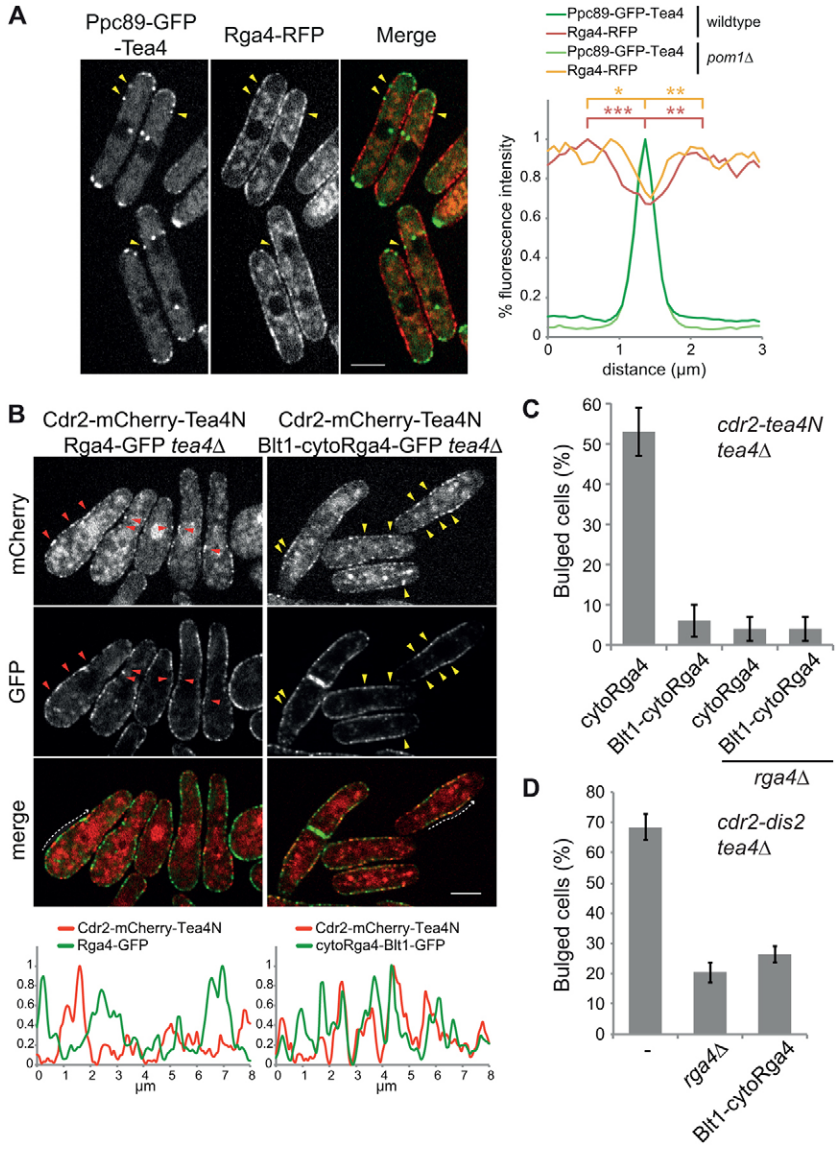

Fig. 6. Rga4 exclusion is required for Tea4-mediated bulge formation. (A) Spinning disk single section image of Ppc89–GFP–Tea4 and Rga4–RFP. Ppc89–GFP–Tea4 dots often lie within regions with low Rga4–RFP signal (arrowheads). A fluorescence line scan over a 3-μm region along the plane of the membrane is shown on the right. ***$P<0.001$, ** $P<0.005$, *$P<0.05$ (Student's *t*-test). (B) Spinning disk confocal single section images of Cdr2–mCherry–Tea4N and Rga4–GFP (left) or Blt1–cytoRga4–GFP (right). Red arrowheads point to regions where Cdr2–mCherry–Tea4N appears to exclude Rga4–GFP. Yellow arrowheads highlight colocalization of Cdr2–mCherry–Tea4N with Blt1–cytoRga4–GFP. A fluorescence line scan, corresponding to the dotted arrow in the images, is shown at the bottom. Similar lines scans were generated for at least six cells. (C) Cdr2–Tea4N-mediated bulge formation in *tea4Δ* cells is blocked by Blt1–cytoRga4, but not by cytoRga4. (D) Cdr2–Dis2-mediated bulge formation in *tea4Δ* cells is reduced in *rga4Δ* and by Blt1–cytoRga4 expression. Results in C and D are means±s.d. Scale bars: 5 μm.

manipulation of yeast cell shape in micro-chambers, that microtubules are key determinants to position sites of polarity, as microtubules contacting cell sides promote the local deposition of polarity factors and, in some conditions, growth (Terenna et al., 2008; Minc et al., 2009). However, this ectopic side-growth was independent of *tea1* (Minc et al., 2009), raising the question of whether the Tea1–Tea4 complex is truly instructive for growth. The Cdr2–Tea4N fusion, which targets the N-terminal part of Tea4 to cell sides, promotes Cdc42 activation and growth at the cell middle, demonstrating that Tea4 is an instructive factor. We conclude that Tea4 is a landmark protein able to recruit the polarization machinery.

Remarkably, in its role as a landmark, Tea4 does not strictly require For3 or Pom1 to promote ectopic growth. Instead, it needs to bind one of the type I phosphatase catalytic subunits Dis2 or Sds21 (Alvarez-Tabarés et al., 2007; Hachet et al., 2011). In addition, ectopic Dis2 or Sds21 behaved similarly to ectopic Tea4 to promote ectopic growth. As both Dis2 and Sds21 can promote growth when targeted to the cell middle, this raises the question of what defines their substrate specificity. The regulatory subunit Tea4 is unlikely to confer specificity, as we showed it is not required for Dis2 and Sds21 activity. Specifically, Tea4 is dispensable for the membrane association of Pom1 upon ectopic cortical Dis2 localization. Rather the sole crucial role of Tea4 is as a targeting device to regulate PP1 localization. Specificity might thus be primarily provided by spatial regulation, in this case proximity to the plasma membrane. In analogy to the role of the phosphatase for Pom1 localization (Hachet et al., 2011), PP1 presence at any plasma membrane site might control the phosphorylation-dependent local attachment (or detachment) of other peripheral membrane proteins.

Recruitment of a Cdc42 GEF and local exclusion of a Cdc42 GAP

We showed that Tea4 promotes Cdc42 activation. Given that CRIB–GFP can be detected on the sides of cells that do not yet display a bulge, this activation occurs before growth. Because Cdc42 activation on cell sides depends on *gef1*, and Gef1 is recruited to cell sides upon ectopic localization of either Tea4 or Dis2, these data suggest that the Tea4–PP1 phosphatase normally recruits Gef1 to cell poles for Cdc42 activation (Fig. 7).

Journal of Cell Science (2014) 127, 2005–2016 doi:10.1242/jcs.142174

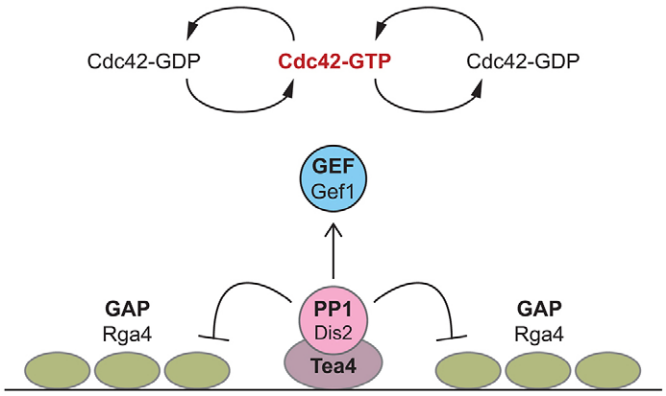

Fig. 7. Model for how the Tea4–Dis2 phosphatase landmark promotes local Cdc42 activation. Tea4–Dis2 phosphatase at the cell cortex promotes the recruitment of Gef1 GEF and the local exclusion of Rga4 GAP. Gef1 recruitment permits the activation of Cdc42, and Rga4 in surrounding regions ensures this activation remains localized.

This positive action of Tea4–PP1 on Gef1 is, however, unlikely to be sufficient, as *gef1Δ* cells exhibit delayed NETO, but eventually grow in a bipolar manner (Coll et al., 2003). We propose that Tea4–Dis2 also favors local Cdc42 activation by promoting the local exclusion of the GAP Rga4 from the cell cortex. Indeed, Ppc89–Tea4 formed cortical dots that correlated with a local low in Rga4 intensity. We cannot exclude, however, that, for unknown reasons, Ppc89–Tea4 dots might simply form preferentially in regions with low Rga4. Remarkably, although Rga4 is required for Tea4- or Dis2-mediated ectopic growth, forced colocalization of Rga4 with ectopic Tea4 or Dis2 prevented ectopic growth. These data suggest that Rga4 must be present, but at sites distinct from Tea4–Dis2, to permit ectopic growth.

These data suggest that the type I phosphatase Dis2 and its targeting device Tea4 promote Cdc42 activation through a dual action: (1) by recruiting the Cdc42 GEF Gef1 for Cdc42 activation, and (2) by excluding the Cdc42 GAP Rga4, thus creating a local decrease in Cdc42 inhibition, concentrating Cdc42 activation to a local zone (Fig. 7). The precise mechanisms by which the phosphatase activity controls the localization and/or activity of Gef1 and Rga4 remain to be investigated, but these results provide a direct link between the landmark and Cdc42 activation. The detected association of Rga4 with Tea4 by co-immunoprecipitation might capture a transient interaction between the phosphatase complex and its substrate. It is remarkable that in *rga4Δ* cells, ectopic Tea4 activates Cdc42, likely through Gef1, yet fails to concentrate it into a bulge. This more-spread localization of active Cdc42 might contribute to more isotropic growth, resulting in the wider shape of *rga4Δ* cells. Thus, the exclusion of Rga4 by Tea4–Dis2 might serve to create a difference in GAP activity between Tea4–Dis2 sites and surrounding regions. We propose that this difference creates a local bias in favor of Cdc42 activation and concentrates Cdc42 activation to a defined region for polarized growth. This represents, to our knowledge, a novel way by which a landmark might indirectly promote cell polarization, in conjunction with direct recruitment of positive factors.

Role of For3 in NETO

We have previously proposed that For3 recruitment by Tea4 serves to initiate bipolar growth, as forced For3 localization to both cell poles promoted bipolar growth in *tea4Δ* and pre-NETO cells (Martin et al., 2005). However, we showed here that For3 is not required for the Tea4-mediated ectopic growth on cell sides. This is perhaps not surprising as, in fission yeast, actin cables are not strictly required for polarized exocytosis and growth. Indeed, polarized growth can be achieved either by vesicle transport along actin cables or by vesicle tethering at cell poles by the exocyst complex (Bendezú and Martin, 2011; Nakano et al., 2011; Snaith et al., 2011). Thus, For3 is likely sufficient, but not strictly required to transduce the landmark function of Tea4 into recruitment of the polarization machinery.

For3 might also be regulated by Tea4–Dis2 phosphatase activity, because Tea4-overexpression-mediated formation of actin cables *in vivo* requires Dis2 binding (Martin et al., 2005; Alvarez-Tabarés et al., 2007). By contrast, the Tea4 homolog in budding yeast, Bud14, binds and regulates the formin Bnr1 independently of its function as a PP1 Glc7 regulatory subunit (Chesarone et al., 2009). It is thus also possible that Tea4 might have phosphatase-independent functions in formin regulation.

Role of Pom1 in cell morphogenesis

The phenotypes that are present in both *tea4Δ* and *pom1Δ* mutants, and the dependency of Pom1 localization on the Tea4–Dis2 phosphatase (Mata and Nurse, 1997; Bähler and Pringle, 1998; Martin et al., 2005; Tatebe et al., 2005; Celton-Morizur et al., 2006; Padte et al., 2006; Huang et al., 2007; Hachet et al., 2011) could have suggested that Pom1 acts as the main or sole effector of the Tea4 complex for cell morphogenesis. However, our results indicate the reality is more complex: Pom1 is not strictly required for Tea4-mediated ectopic growth and cannot promote bipolar growth when present at cell tips in absence of functional Tea4. In addition, Pom1 does not appear to act as a landmark, as it was unable to promote ectopic growth when localized along cell sides, although it is possible that we were not able to target sufficient amounts of Pom1 to cell sides. Collectively, these data suggest Pom1 is not instructive, but a permissive factor required for Tea4 function.

However, because *pom1* is required for bipolar growth, as well as for restriction of Rga4 from the non-growing cell pole, it performs a crucial function in allowing the landmark to recruit the polarization machinery. One possibility is that Pom1 favors the effects of Tea4, for instance by promoting the exclusion of Rga4 (Tatebe et al., 2008). Another, which would explain its more important role at cell poles than at sites of ectopic Tea4–Dis2, is that it is involved in feedback regulation of Tea4 at the cell poles, which becomes dispensable in our ectopic growth assay. This idea remains to be investigated.

Polarizing at cell tips and NETO

How do our data dissecting the ability of Tea4 to promote ectopic growth on cell sides relate to its normal function at cell tips? Polarized growth at cell tips is robust, due in part to positive-feedback mechanisms. In addition, the curvature of cell poles, as well as their growth history, might distinguish these locations from cell sides to promote growth positioning there. The ectopic Tea4 assay described in this bypasses these feedback, geometric and historical mechanisms and permits dissecting out the direct function of the landmark.

We propose that, at cell poles, Tea4–PP1 recruits the Cdc42 polarization machinery by making multiple connections: by recruiting Gef1 and excluding Rga4, as well as by recruiting For3 and Pom1, which in turn contributes to Rga4 exclusion (Martin

Journal of Cell Science (2014) 127, 2005–2016 doi:10.1242/jcs.142174

et al., 2005; Tatebe et al., 2008). Connections with the endocytic machinery have also been proposed (Castagnetti et al., 2005; Snaith et al., 2011). It is also possible that other Cdc42 activators, such as the GEF Scd1 or scaffold Scd2, are directly recruited by Tea4, but their strong involvement in cell polarization per se precluded their investigation here. Other Cdc42 GAPs might also exist amongst the eight predicted GAPs in the *S. pombe* genome (Nakano et al., 2001). In agreement with the idea that multiple connections between the landmark and the polarization machinery contribute to robust polarized growth, the *tea4*^{SH3*} allele, which blocks Dis2 and Pom1 binding but is not predicted to affect For3 interaction (Martin et al., 2005), has a weaker phenotype than *tea4Δ*. The *tea4*^{RVxF*} allele, which blocks only Dis2 binding, has an even weaker phenotype (Alvarez-Tabarés et al., 2007; and our unpublished data). Similarly, deletion of *rga4Δ*, like *gef1Δ* or *for3Δ*, has modest effects on NETO and these cells do not form T-shapes, in contrast to *tea4Δ* cells, which are severely monopolar and form T-shapes upon re-growth (Feierbach and Chang, 2001; Coll et al., 2003; Das et al., 2007).

One longstanding question is that of the signal for NETO. As Tea4–PP1 is present at both cell tips even in pre-NETO cells, this landmark is unlikely to form the signal for NETO. The NETO signal is likely emitted remotely from the spindle pole body through an intermediate increase in CDK1 activity at mid-G2 phase (Grallert et al., 2013). Interestingly, in *S. cerevisiae* and *C. albicans* the Cdc42 GAP Rga2 is phosphorylated by CDK1 to regulate its localization and activation (Sopko et al., 2007; Zheng et al., 2007). In *S. pombe*, Rga4 is highly phosphorylated, with 21 potential CDK phosphorylation sites (Tatebe et al., 2008). As Cdc42 and its regulators oscillate from pole to pole even in pre-NETO cells (Bendezú and Martin, 2012; Das et al., 2012), some of these might transit through the cytosol throughout interphase. It is thus possible that these are targets of the NETO signal in the cytosol, which could mark them for dephosphorylation by Tea4–Dis2.

MATERIALS AND METHODS

Yeast strains and genetic manipulations

Standard methods were used for fission yeast media and genetic manipulations. Tagged and deletion strains were constructed by using a PCR-based approach (Bähler and Pringle, 1998). All strains are listed in supplementary material Table S1. All strains were grown in Edinburgh minimal medium (EMM) with appropriate supplements, except for the re-feeding experiments in Fig. 3E, which were grown in yeast extract medium (YE).

Strains expressing Cdr2–Tea4N or Cdr2–Dis2 fusions were generated as follows. We generated pRIP81-based plasmids encoding, in this order, amino acids 1–774 of Cdr2, a GS linker, GFP or CFP or mCherry, and a PGAGAGAGS linker and amino acids 1–521 of Tea4 followed by a TAG stop codon, or a PGK linker and amino acids 1–327 of Dis2, or a PGK linker and amino acids 1–322 of Sds21, under control of the *nmt81* promoter. The *tea4*^{RVxF*} allele has mutation *222-225RVXF-RAXA*; the *tea4*^{SH3*} allele has mutation *W155A-W156A* (Hachet et al., 2011). The *dis2*^{H247K} allele has mutation H247K, in which one of the histidine residues coordinating an essential catalytic metal ion is mutated (Egloff et al., 1995; Goldberg et al., 1995). These mutations were introduced by site-directed mutagenesis. These plasmids were sequenced and linearized within the *ura4+* open reading frame (ORF), with either StuI or AvrII, transformed into an *ura4-294* strain and stable insertions selected. All three Cdr2–Tea4N fusions (Cdr2–GFP–Tea4N, Cdr2–CFP–Tea4N, Cdr2–mCherry–Tea4N) led to the same phenotype (data not shown), and were thus used interchangeably.

To generate the strain leu1-32::shk1 promoter ScGIC2 CRIB:GFP3:leu1+, the *S. pombe leu1* gene was amplified with primers with *Sal*I extension and cloned at the *Sal*I site of a pBluescript SK+ plasmid, containing the shk1 promoter:ScGIC2 CRIB-3GFP (Tatebe et al., 2008). This was then linearized plasmid with *Nru*I, transformed in a *leu1-32* strain and stable insertions were selected.

Microscopy

Microscopy was performed at room temperature on live cells by using generally one of two microscopes: an inverted spinning disk microscope consisting of a Leica DMI4000B inverted microscope equipped with an HCX PL APO 100×/1.46 NA oil objective and a PerkinElmer Ultraview confocal system (including a Yokagawa CSU22 real-time confocal scanning head, an argon/krypton laser, and a cooled 14-bit frame transfer EMCCD C9100-50 camera), or a DeltaVision system composed of a customized Olympus IX-71 inverted microscope stand fitted with a Plan Apo 60× or 100×/1.42 NA oil objective, a CoolSNAP HQ2 camera, and an Insight SSI 7 color combined unit illuminator. Images were acquired with Volocity or softWoRx softwares, respectively. Fig. 1B; Fig. 2A,B (all but Scd1–3GFP); Fig. 2C–G; Fig. 3A,D (Pom1–Mid1C–mCherry); Fig. 3F; Fig. 4B,D; Fig. 5C,E; and Fig. 6A,B were acquired on the spinning disk; Fig. 1C,D; Fig. 2B (Scd1–3GFP); Fig. 3D (Pom1–Cdr2–GFP and Pom1–Cdr2C–GFP); and Fig. 4A were acquired on the DeltaVision system. Of these, panels Fig. 1C, Fig. 2B and Fig. 4A were further deconvolved. Images in Fig. 5B were acquired on a wide-field Leica AF6000 system consisting of a DM6000B upright microscope fitted with a 63×/0.75 NA objective, a Leica DFC350× CCD camera, a Leica EL6000 light source and Chrome filter sets.

nmt81-cdr2-tea4N, *nmt81-cdr2-dis2* or *nmt81-cdr2-sds21* fusions expressions were induced for 28 h–32 h to steady-state levels in absence of thiamine in EMM, except for imaging of rod-shaped cells, where fusion expression was induced for 18–20 h. For time-lapse microscopy, fusions were induced for 20–24 h in EMM, reaching log-phase and then diluted to an optical density (OD) of 0.1. 100 µl of cells were loaded in ONIX microfluidic chambers (Y04C plates, CellAsic) in EMM with a flux rate of 2 psi for 60 s and then of 8 psi for 5 s for three times. Afterwards, the flow rate was kept constant at 2 psi for the rest of the time-lapse experiment. Actin stainings were performed as described previously (Bendezú and Martin, 2011). For lectin stainings, cells were stained with 10 µg/ml tetramethylrhodamine B isothiocyanate (TRITC)–lectin (stock of 5 mg/ml in distilled H_2O, Sigma) for 15 min. Cells were then washed twice, resuspended in EMM, diluted to OD_{600}=0.2 in EMM and grown for 1 h before being stained with Calcofluor White from 200× stock (2 mg/ml in 100 mM Tris-HCl, pH 9.0). Images shown are single medial sections or maximum projection of two or three medial sections, except where specified. Figures were prepared with ImageJ and Adobe Illustrator CS3.

Measurements

For measurement of fluorescence intensity along the cell cortex, a 3-pixel-wide line was drawn by hand at the cell periphery in a medial section image, fluorescence intensity obtained using the plot profile tool of ImageJ, and background signal measured outside the cell was subtracted. Monopolar growth was evaluated on septated cells. Septum position was calculated by taking the ratio of the distance between the septum and the cell end furthest away and the total cell length. In all quantifications, 100 or more cells were counted in three distinct experiments. For the quantification of protein localization shown in Fig. 2 and supplementary material Table S2, only interphase cells were quantified. Anaphase and cytokinetic cells, which could be identified by the shape and number of nuclei, were excluded from the analysis. In addition, in most cases, the medial signal was observed only on one side of the cell or was otherwise asymmetric, distinct from the normal medial recruitment of some of these factors at cytokinesis. All measurements and calculations were performed in ImageJ and Microsoft Excel, respectively.

Biochemistry

For TAP purification of Tea4-TAP and Tea4^{SH3}-TAP, extracts from yeast grown in YE5S or in EMM medium containing the required supplements were prepared in CXS buffer (50 mM Hepes pH 7.0, 150 mM KCl, 1 mM $MgCl_2$, 2 mM EDTA and protease inhibitor cocktail) by grinding

in liquid nitrogen with mortar and pestle as described previously (Feierbach et al., 2004). During thawing PMSF and protease inhibitor cocktail were added to a final concentration of 1% and 0.1% respectively. After thawing samples were spinned in a table centrifuge at 13 krpm for 5 min at 4℃. The supernatant was collected and Tris-HCl pH 8.0, NaCl and NP-40 were added to a final concentration of 10 mM, 150 mM and 0.1%, respectively, and high-speed soluble extracts were prepared by centrifugation at 45 krpm (180,000 ***g***) for 30 min in the S100-3 rotor (Beckman). 600 µl of dynabeads conjugated to Protein G (Invitrogen) were incubated with 200 µg rabbit IgG (Sigma) for 1 h at room temperature with rotation, and the beads were washed once with 1 ml cold 1× PBS and twice with 1 ml cold IPP150 (10 mM Tris-HCl pH 8.0, 150 mM NaCl, 0.5 mM EDTA, 0.1% NP-40). Soluble extracts (corresponding to ∼3 l of log-phase culture) were added to the beads and incubated for 2 h at 4℃. Beads were washed 7× with 1 ml cold IPP150 buffer, 1× in 1 ml cold TEV buffer (10 mM Tris-HCl pH 8.0, 150 mM NaCl, 0.5 mM EDTA, 0.01% NP-40) and incubated for 1.5 h at room temperature in 500 µl TEV buffer plus 1 mM DTT and 20 µl TEV protease (Invitrogen). The supernatant was TCA-precipitated, dried and analyzed by mass spectrometry (see below).

For Rga4–GFP co-immunoprecipitation with Tea4–HA–Protein-A, extracts from ∼150 ml log-phase yeast culture grown in EMM medium were prepared in CXS buffer (50 mM Hepes pH 7.0, 150 mM KCl, 1 mM MgCl2, 2 mM EDTA and protease inhibitor cocktail) by grinding in liquid nitrogen with mortar and pestle. During thawing 1% PMSF and protease inhibitor cocktail were added. After thawing, samples were spinned in a table centrifuge at 13 krpm (15,700 ***g***) for 5 min at 4℃. The supernatant was collected and Tris-HCl pH 8.0, NaCl and NP-40 were added to a final concentration of 10 mM, 150 mM and 0.1%, respectively, and high-speed soluble extracts were prepared by centrifugation at 45 krpm (180,000 ***g***) for 30 min in the S100-3 rotor (Beckman). 400 µl soluble extract was added to 50 µl dynabeads conjugated to Protein G (Invitrogen) pre-bound to 300 µg rabbit IgG (Sigma) and incubated for 2 h at 4℃. After incubation, the beads were washed seven times with 1 ml cold IPP150 buffer (10 mM Tris-HCl pH 8.0, 150 mM NaCl, 0.1% NP-40, 1 mM $MgCl_2$, 2 mM EDTA), 1×in 1 ml cold TEV buffer (10 mM Tris-HCl pH 8.0, 150 mM NaCl, 0.5 mM EDTA, 0.01% NP-40, 0.01% Tween 20) and incubated for 45 min at room temperature with regular mixing (every 10 min) in 28 µl TEV buffer plus 1 mM DTT and 1.7 µl TEV protease (Invitrogen). The supernatant (30 µl) was removed and 28 µl TEV buffer plus 1 mM DTT and 1.7 µl TEV protease was further added and incubated for 45 min at room temperature with regular mixing (every 10 minutes). Both supernatants combined and 30 µl 3× sample buffer were boiled and analyzed by SDS-PAGE and western blotting. Antibodies used on western blots were mouse monoclonal anti-GFP (1:2000) (Roche) and anti-HA.11 (1:1000) (Covance).

Mass spectrometry

Samples were migrated on a mini polyacrylamide gel for about 2 cm, and stained with Coomassie Blue. Entire gel lanes were excised into five equal regions from top to bottom and digested with trypsin (Promega) as described previously (Shevchenko et al., 1996; Wilm et al., 1996). Data-dependent liquid chromatography tandem mass spectrometry (LC-MS/MS) analysis of extracted peptide mixtures after digestion with trypsin was carried out on a hybrid linear trap LTQ-Orbitrap mass spectrometer (Thermo Scientific) interfaced to a nanocapillary HPLC equipped with a C18 reversed-phase column (Agilent). Collections of tandem mass spectra for database searching were generated from raw data with Mascot Distiller and searched using Mascot 2.2 (Matrix Science, London, UK) against the release 13.2 of the UniProt database restricted to *Schizosaccharomyces pombe* taxonomy. Mascot was searched with a fragment ion mass tolerance of 0.50 Da and a parent ion tolerance of 10 ppm, allowing one missed cleavage. The iodoacetamide derivative of cysteine was specified as a fixed modification. Deamidation of asparagine and glutamine, and oxidation of methionine were specified as variable modifications. The software Scaffold (version Scaffold-02_00_03, Proteome Software Inc.) was used to validate MS/MS-based peptide [minimum 90% probability (Keller et al., 2002)] and protein [minimum 95% probability (Nesvizhskii et al., 2003)] identifications, and to perform dataset alignment as well as parsimony analysis to discriminate homologous hits.

Acknowledgements

We thank Manfredo Quadroni and Patrice Waridel (Protein Analysis Facility, University of Lausanne, Switzerland) for the mass spectrometry analysis, Felipe Bendezu, Payal and Laura Merlini (Department of Fundamental Microbiology, University of Lausanne, Switzerland) for careful reading of the manuscript and the Martin laboratory for advice and discussion.

Competing interests

The authors declare no competing interests.

Author contributions

S.G.M. conceived of the project. K.K., D.G.C. and S.G.M. designed and performed the experiments. S.G.M. wrote the paper, which was reviewed by all authors.

Funding

This work was supported by a Swiss National Science Foundation (SNF) Professorship grant [grant number PP00A-114936]; a SNF Research grant [grant number 31003A_138177]; and a Roche Research Foundation grant [grant number Mkl/stm 67-2008] all to S.G.M. D.G.C. is supported by a Faculty of Biology and Medicine, University of Lausanne PhD fellowship. Research in the laboratory of S.G.M. is also supported by a European Research Council Starting Grant [grant number 260493].

Supplementary material

Supplementary material available online at
http://jcs.biologists.org/lookup/suppl/doi:10.1242/jcs.142174/-/DC1

References

Alvarez-Tabarés, I., Grallert, A., Ortiz, J. M. and Hagan, I. M. (2007). Schizosaccharomyces pombe protein phosphatase 1 in mitosis, endocytosis and a partnership with Wsh3/Tea4 to control polarised growth. *J. Cell Sci.* **120**, 3589-3601.

Bähler, J. and Pringle, J. R. (1998). Pom1p, a fission yeast protein kinase that provides positional information for both polarized growth and cytokinesis. *Genes Dev.* **12**, 1356-1370.

Bhatia, P., Hachet, O., Hersch, M., Rincon, S. A., Berthelot-Grosjean, M., Dalessi, S., Basterra, L., Bergmann, S., Paoletti, A. and Martin, S. G. (2014). Distinct levels in Pom1 gradients limit Cdr2 activity and localization to time and position division. *Cell Cycle* **13**, 538-552.

Bendezú, F. O. and Martin, S. G. (2011). Actin cables and the exocyst form two independent morphogenesis pathways in the fission yeast. *Mol. Biol. Cell* **22**, 44-53.

Bendezú, F. O. and Martin, S. G. (2012). Cdc42 oscillations in yeasts. *Sci. Signal.* **5**, pe53.

Bendezú, F. O., Vincenzetti, V. and Martin, S. G. (2012). Fission yeast Sec3 and Exo70 are transported on actin cables and localize the exocyst complex to cell poles. *PLoS ONE* **7**, e40248.

Bi, E. and Park, H. O. (2012). Cell polarization and cytokinesis in budding yeast. *Genetics* **191**, 347-387.

Bicho, C. C., Kelly, D. A., Snaith, H. A., Goryachev, A. B. and Sawin, K. E. (2010). A catalytic role for Mod5 in the formation of the Tea1 cell polarity landmark. *Curr. Biol.* **20**, 1752-1757.

Castagnetti, S., Behrens, R. and Nurse, P. (2005). End4/Sla2 is involved in establishment of a new growth zone in Schizosaccharomyces pombe. *J. Cell Sci.* **118**, 1843-1850.

Castagnetti, S., Novák, B. and Nurse, P. (2007). Microtubules offset growth site from the cell centre in fission yeast. *J. Cell Sci.* **120**, 2205-2213.

Celton-Morizur, S., Racine, V., Sibarita, J. B. and Paoletti, A. (2006). Pom1 kinase links division plane position to cell polarity by regulating Mid1p cortical distribution. *J. Cell Sci.* **119**, 4710-4718.

Chang, E. C., Barr, M., Wang, Y., Jung, V., Xu, H. P. and Wigler, M. H. (1994). Cooperative interaction of S. pombe proteins required for mating and morphogenesis. *Cell* **79**, 131-141.

Chesarone, M., Gould, C. J., Moseley, J. B. and Goode, B. L. (2009). Displacement of formins from growing barbed ends by bud14 is critical for actin cable architecture and function. *Dev. Cell* **16**, 292-302.

Coll, P. M., Trillo, Y., Ametzazurra, A. and Perez, P. (2003). Gef1p, a new guanine nucleotide exchange factor for Cdc42p, regulates polarity in Schizosaccharomyces pombe. *Mol. Biol. Cell* **14**, 313-323.

Cortés, J. C., Ishiguro, J., Durán, A. and Ribas, J. C. (2002). Localization of the (1,3)beta-D-glucan synthase catalytic subunit homologue Bgs1p/Cps1p from fission yeast suggests that it is involved in septation, polarized growth, mating, spore wall formation and spore germination. *J. Cell Sci.* **115**, 4081-4096.

Das, M., Wiley, D. J., Medina, S., Vincent, H. A., Larrea, M., Oriolo, A. and Verde, F. (2007). Regulation of cell diameter, For3p localization, and cell symmetry by fission yeast Rho-GAP Rga4p. *Mol. Biol. Cell* **18**, 2090-2101.
Das, M., Wiley, D. J., Chen, X., Shah, K. and Verde, F. (2009). The conserved NDR kinase Orb6 controls polarized cell growth by spatial regulation of the small GTPase Cdc42. *Curr. Biol.* **19**, 1314-1319.
Das, M., Drake, T., Wiley, D. J., Buchwald, P., Vavylonis, D. and Verde, F. (2012). Oscillatory dynamics of Cdc42 GTPase in the control of polarized growth. *Science* **337**, 239-243.
Egloff, M. P., Cohen, P. T., Reinemer, P. and Barford, D. (1995). Crystal structure of the catalytic subunit of human protein phosphatase 1 and its complex with tungstate. *J. Mol. Biol.* **254**, 942-959.
Estravís, M., Rincón, S. A., Santos, B. and Pérez, P. (2011). Cdc42 regulates multiple membrane traffic events in fission yeast. *Traffic* **12**, 1744-1758.
Feierbach, B. and Chang, F. (2001). Roles of the fission yeast formin for3p in cell polarity, actin cable formation and symmetric cell division. *Curr. Biol.* **11**, 1656-1665.
Feierbach, B., Verde, F. and Chang, F. (2004). Regulation of a formin complex by the microtubule plus end protein tea1p. *J. Cell Biol.* **165**, 697-707.
Goldberg, J., Huang, H. B., Kwon, Y. G., Greengard, P., Nairn, A. C. and Kuriyan, J. (1995). Three-dimensional structure of the catalytic subunit of protein serine/threonine phosphatase-1. *Nature* **376**, 745-753.
Grallert, A., Patel, A., Tallada, V. A., Chan, K. Y., Bagley, S., Krapp, A., Simanis, V. and Hagan, I. M. (2013). Centrosomal MPF triggers the mitotic and morphogenetic switches of fission yeast. *Nat. Cell Biol.* **15**, 88-95.
Gulli, M. P., Jaquenoud, M., Shimada, Y., Niederhäuser, G., Wiget, P. and Peter, M. (2000). Phosphorylation of the Cdc42 exchange factor Cdc24 by the PAK-like kinase Cla4 may regulate polarized growth in yeast. *Mol. Cell* **6**, 1155-1167.
Hachet, O., Berthelot-Grosjean, M., Kokkoris, K., Vincenzetti, V., Moosbrugger, J. and Martin, S. G. (2011). A phosphorylation cycle shapes gradients of the DYRK family kinase Pom1 at the plasma membrane. *Cell* **145**, 1116-1128.
Hachet, O., Bendezú, F. O. and Martin, S. G. (2012). Fission yeast: in shape to divide. *Curr. Opin. Cell Biol.* **24**, 858-864.
Harris, K. P. and Tepass, U. (2010). Cdc42 and vesicle trafficking in polarized cells. *Traffic* **11**, 1272-1279.
Hirota, K., Tanaka, K., Ohta, K. and Yamamoto, M. (2003). Gef1p and Scd1p, the Two GDP-GTP exchange factors for Cdc42p, form a ring structure that shrinks during cytokinesis in Schizosaccharomyces pombe. *Mol. Biol. Cell* **14**, 3617-3627.
Huang, Y., Chew, T. G., Ge, W. and Balasubramanian, M. K. (2007). Polarity determinants Tea1p, Tea4p, and Pom1p inhibit division-septum assembly at cell ends in fission yeast. *Dev. Cell* **12**, 987-996.
Irazoqui, J. E., Gladfelter, A. S. and Lew, D. J. (2003). Scaffold-mediated symmetry breaking by Cdc42p. *Nat. Cell Biol.* **5**, 1062-1070.
Johnson, J. M., Jin, M. and Lew, D. J. (2011). Symmetry breaking and the establishment of cell polarity in budding yeast. *Curr. Opin. Genet. Dev.* **21**, 740-746.
Keller, A., Nesvizhskii, A. I., Kolker, E. and Aebersold, R. (2002). Empirical statistical model to estimate the accuracy of peptide identifications made by MS/MS and database search. *Anal. Chem.* **74**, 5383-5392.
Kelly, F. D. and Nurse, P. (2011). Spatial control of Cdc42 activation determines cell width in fission yeast. *Mol. Biol. Cell* **22**, 3801-3811.
Martin, S. G. (2009). Microtubule-dependent cell morphogenesis in the fission yeast. *Trends Cell Biol.* **19**, 447-454.
Martin, S. G. and Berthelot-Grosjean, M. (2009). Polar gradients of the DYRK-family kinase Pom1 couple cell length with the cell cycle. *Nature* **459**, 852-856.
Martin, S. G. and Chang, F. (2005). New end take off: regulating cell polarity during the fission yeast cell cycle. *Cell Cycle* **4**, 4046-4049.
Martin, S. G., McDonald, W. H., Yates, J. R., III and Chang, F. (2005). Tea4p links microtubule plus ends with the formin for3p in the establishment of cell polarity. *Dev. Cell* **8**, 479-491.
Martin, S. G., Rincón, S. A., Basu, R., Pérez, P. and Chang, F. (2007). Regulation of the formin for3p by cdc42p and bud6p. *Mol. Biol. Cell* **18**, 4155-4167.
Mata, J. and Nurse, P. (1997). tea1 and the microtubular cytoskeleton are important for generating global spatial order within the fission yeast cell. *Cell* **89**, 939-949.
Miller, P. J. and Johnson, D. I. (1994). Cdc42p GTPase is involved in controlling polarized cell growth in Schizosaccharomyces pombe. *Mol. Cell. Biol.* **14**, 1075-1083.
Minc, N., Bratman, S. V., Basu, R. and Chang, F. (2009). Establishing new sites of polarization by microtubules. *Curr. Biol.* **19**, 83-94.
Mitchison, J. M. and Nurse, P. (1985). Growth in cell length in the fission yeast Schizosaccharomyces pombe. *J. Cell Sci.* **75**, 357-376.
Morrell, J. L., Nichols, C. B. and Gould, K. L. (2004). The GIN4 family kinase, Cdr2p, acts independently of septins in fission yeast. *J. Cell Sci.* **117**, 5293-5302.
Moseley, J. B., Mayeux, A., Paoletti, A. and Nurse, P. (2009). A spatial gradient coordinates cell size and mitotic entry in fission yeast. *Nature* **459**, 857-860.
Nakano, K., Mutoh, T. and Mabuchi, I. (2001). Characterization of GTPase-activating proteins for the function of the Rho-family small GTPases in the fission yeast Schizosaccharomyces pombe. *Genes Cells* **6**, 1031-1042.
Nakano, K., Toya, M., Yoneda, A., Asami, Y., Yamashita, A., Kamasawa, N., Osumi, M. and Yamamoto, M. (2011). Pob1 ensures cylindrical cell shape by coupling two distinct rho signaling events during secretory vesicle targeting. **12**, 726-739.
Nesvizhskii, A. I., Keller, A., Kolker, E. and Aebersold, R. (2003). A statistical model for identifying proteins by tandem mass spectrometry. *Anal. Chem.* **75**, 4646-4658.
Ohkura, H., Kinoshita, N., Miyatani, S., Toda, T. and Yanagida, M. (1989). The fission yeast dis2+ gene required for chromosome disjoining encodes one of two putative type 1 protein phosphatases. *Cell* **57**, 997-1007.
Padte, N. N., Martin, S. G., Howard, M. and Chang, F. (2006). The cell-end factor pom1p inhibits mid1p in specification of the cell division plane in fission yeast. *Curr. Biol.* **16**, 2480-2487.
Rincón, S. A., Ye, Y., Villar-Tajadura, M. A., Santos, B., Martin, S. G. and Pérez, P. (2009). Pob1 participates in the Cdc42 regulation of fission yeast actin cytoskeleton. *Mol. Biol. Cell* **20**, 4390-4399.
Sawin, K. E. and Snaith, H. A. (2004). Role of microtubules and tea1p in establishment and maintenance of fission yeast cell polarity. *J. Cell Sci.* **117**, 689-700.
Shevchenko, A., Wilm, M., Vorm, O. and Mann, M. (1996). Mass spectrometric sequencing of proteins silver-stained polyacrylamide gels. *Anal. Chem.* **68**, 850-858.
Slaughter, B. D., Smith, S. E. and Li, R. (2009). Symmetry breaking in the life cycle of the budding yeast. *Cold Spring Harb. Perspect. Biol.* **1**, a003384.
Snaith, H. A. and Sawin, K. E. (2003). Fission yeast mod5p regulates polarized growth through anchoring of tea1p at cell tips. *Nature* **423**, 647-651.
Snaith, H. A., Thompson, J., Yates, J. R., III and Sawin, K. E. (2011). Characterization of Mug33 reveals complementary roles for actin cable-dependent transport and exocyst regulators in fission yeast exocytosis. *J. Cell Sci.* **124**, 2187-2199.
Sopko, R., Huang, D., Smith, J. C., Figeys, D. and Andrews, B. J. (2007). Activation of the Cdc42p GTPase by cyclin-dependent protein kinases in budding yeast. *EMBO J.* **26**, 4487-4500.
Tatebe, H., Shimada, K., Uzawa, S., Morigasaki, S. and Shiozaki, K. (2005). Wsh3/Tea4 is a novel cell-end factor essential for bipolar distribution of Tea1 and protects cell polarity under environmental stress in S. pombe. *Curr. Biol.* **15**, 1006-1015.
Tatebe, H., Nakano, K., Maximo, R. and Shiozaki, K. (2008). Pom1 DYRK regulates localization of the Rga4 GAP to ensure bipolar activation of Cdc42 in fission yeast. *Curr. Biol.* **18**, 322-330.
Terenna, C. R., Makushok, T., Velve-Casquillas, G., Baigl, D., Chen, Y., Bornens, M., Paoletti, A., Piel, M. and Tran, P. T. (2008). Physical mechanisms redirecting cell polarity and cell shape in fission yeast. *Curr. Biol.* **18**, 1748-1753.
Thompson, B. J. (2013). Cell polarity: models and mechanisms from yeast, worms and flies. *Development* **140**, 13-21.
Umesono, K., Toda, T., Hayashi, S. and Yanagida, M. (1983). Cell division cycle genes nda2 and nda3 of the fission yeast Schizosaccharomyces pombe control microtubular organization and sensitivity to anti-mitotic benzimidazole compounds. *J. Mol. Biol.* **168**, 271-284.
Wedlich-Soldner, R., Altschuler, S., Wu, L. and Li, R. (2003). Spontaneous cell polarization through actomyosin-based delivery of the Cdc42 GTPase. *Science* **299**, 1231-1235.
Wilm, M., Shevchenko, A., Houthaeve, T., Breit, S., Schweigerer, L., Fotsis, T. and Mann, M. (1996). Femtomole sequencing of proteins from polyacrylamide gels by nano-electrospray mass spectrometry. *Nature* **379**, 466-469.
Zheng, X. D., Lee, R. T., Wang, Y. M., Lin, Q. S. and Wang, Y. (2007). Phosphorylation of Rga2, a Cdc42 GAP, by CDK/Hgc1 is crucial for Candida albicans hyphal growth. *EMBO J.* **26**, 3760-3769.

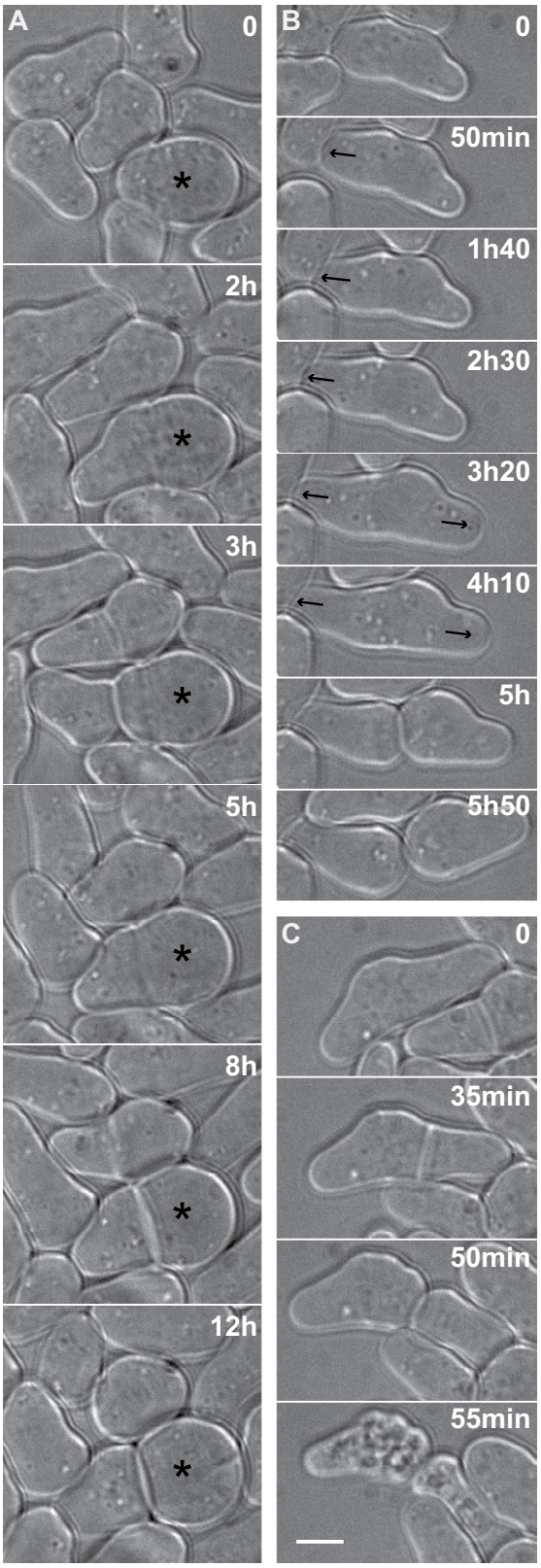

Fig. S1: Growth of bulged cells

Timelapse transmitted light images of tea4Δ cdr2-GFP-tea4N cells grown in a flow-chamber.

A: Example of cell rounding over time (asterisk).

B: Example of bipolar growth (arrows).

C: Example of cells dying shortly after cell division. Scale bar is 5µm.

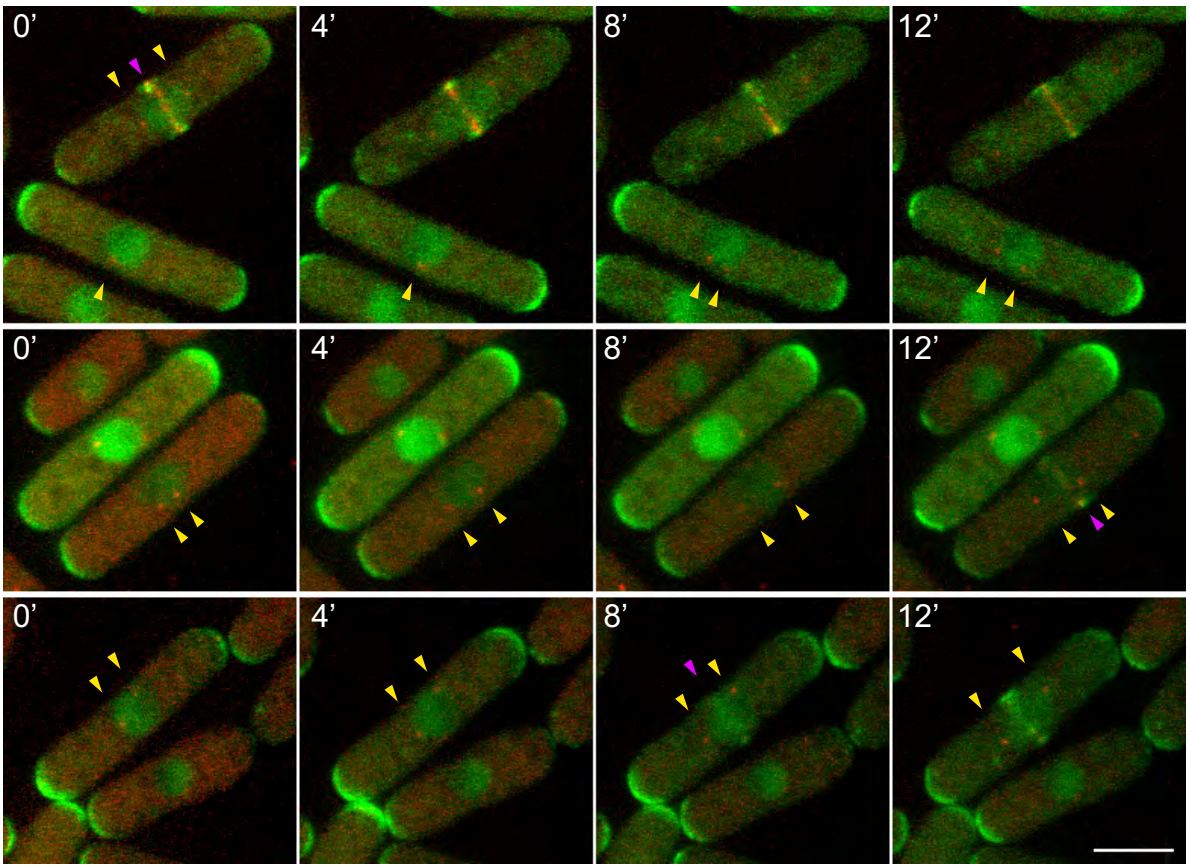

Fig. S2. Localization of CRIB and Gef1 in wildtype cells

Three timelapse sequences of CRIB-3GFP and Gef1-tdTomato in cells co-expressing Sid4-mRFP to indicate spindle pole body separation at mitotic entry. CRIB and Gef1 do not localize to the cell middle of interphase or early mitotic cells and only appear at the future division site in cells with early anaphase spindles of about 3µm in length. Time is shown in min.

Movie 1. Growth of bulged cells

Timelapse transmitted light images of tea4Δ cdr2-GFP-tea4N cells grown in EMM in a flow-chamber. Cells were imaged every 5 min. The timelapse is sped up 2100x.

Supplementary Table 1: Strains used in this study

Number	Genotype	Source
Fig. 1		
YSM1683	h+ ura4-294::nmt81:cdr2-GFP-tea4N-ura4+ ade6+ leu1-32	This study
YSM2251	h+ ura4-294::nmt81:cdr2-GFP-tea4N-ura4+ tea4Δ::kanMX ade6-M216 leu1-32	This study
Fig. 2		
YSM2253	ura4-294::nmt81:cdr2-mCherry-Tea4N-ura4+ tea4Δ::kanMX dis2-NEGFP-ura4+ ade6- leu1-32	This study
YSM2254	ura4-294::nmt81:cdr2-mCherry-Tea4N-ura4+ tea4Δ::kanMX pom1-GFP-kanMX ade6- leu1-32	This study
YSM2255	ura4-294::nmt81:cdr2-mCherry-Tea4N-ura4+ tea4Δ::kanMX for3-3GFP-ura4+ ade6- leu1-32	This study
YSM2256	ura4-294::nmt81:cdr2-mCherry-ura4+ tea4Δ::kanMX tea1- GFP::kanMX ade6- leu1-	This study
YSM2257	ura4-294::nmt81:cdr2-mCherry-Tea4N-ura4+ tea4Δ::kanMX tea1-GFP::kanMX ade6- leu1-32	This study
YSM2258	ura4-294::nmt81:cdr2-mCherry-Tea4N-ura4+ tea4Δ::kanMX scd1-3GFP-ura4+ ade6- leu1-32	This study
YSM2259	ura4-294::nmt81:cdr2-mCherry-ura4+ tea4Δ::kanMX pom1- GFP-kanMX ade6- leu1-32	This study
YSM2260	ura4-294::nmt81:cdr2-mCherry-ura4+ tea4Δ::kanMX dis2-NEGFP-ura4+ ade6- leu1-32	This study
YSM2261	ura4-294::nmt81:cdr2-mCherry-ura4+ tea4Δ::kanMX for3-3GFP-ura4+ ade6- leu1-32	This study
YSM2262	ura4-294::nmt81:cdr2-mCherry-ura4+ tea4Δ::kanMX scd1- 3GFP-ura4+ ade6- leu1-32	This study
YSM2263	ura4-294::nmt81:cdr2-mCherry-tea4N-ura4+ tea4Δ::kanMX exo70-GFP-ura4+ ade6- leu1-32	This study
YSM2264	ura4-294::nmt81:cdr2-mCherry-ura4+ tea4Δ::kanMX exo70- GFP-ura4+ ade6- leu1-32	This study
YSM2265	ura4-294::nmt81:cdr2-mCherry-Tea4N-ura4+ tea4Δ::kanMX pSV40-atb2GFP-leu+ ade6-	This study
YSM2266	h- ura4-294::nmt81:cdr2-mCherry-ura4+ tea4Δ::kanMX leu1- 32::shk1 promoter:ScGIC2 CRIB:GFP3:leu1+ ade6-	This study
YSM2267	h- ura4-294::nmt81:cdr2-mCherry-Tea4N-ura4+ tea4Δ::kanMX leu1-32::shk1 promoter:ScGIC2 CRIB:GFP3:leu1+ ade6-	This study
YSM2268	h- ura4-294::nmt81:cdr2-CFP-tea4N-ura4+ tea4Δ::kanMX gef1-GFP-kanMX ade6- leu1-32	This study
YSM2269	h+ ura4-294::nmt81:cdr2-CFP-ura4+ tea4Δ::kanMX gef1-GFP-kanMX ade6- leu1-32	This study
YSM2331	myo52-tdTomato-natMX ura4-294::nmt81:cdr2-GFP-ura4+ tea4Δ::kanMX ade6? leu1-32	This study
YSM2332	myo52-tdTomato-natMX ura4-294::nmt81:cdr2-GFP-tea4N-ura4+ tea4Δ::kanMX ade6? leu1-32	This study
Fig. 3		
YSM2251	h+ ura4-294::nmt81:cdr2-GFP-tea4N-ura4+ tea4Δ::kanMX ade6-M216 leu1-32	This study
YSM2273	h- tea4Δ::kanMX ura4-294::nmt81:cdr2-GFP-tea4N^{RVxF*}-ura4+ ade6? leu1-32	This study
YSM2274	tea4Δ::kanMX ura4-294::nmt81:cdr2-GFP-tea4N^{SH3*}-ura4+ ade6? leu1-32	This study
YSM1182	h+ ade6-M216 leu1-32 ura4-D18	Lab stock
YSM2270	h- tea4^{SH3*} ade6-M216 leu1-32 ura4-D18	This study
YSM2271	h+ pom1^{6A}-GFP ade6-M216 leu1-32 ura4-D18	Hachet et al, 2011
YSM2272	tea4WW155-156AA pom1Psites to A (1,2,3,4,5,8)-GFP- KanMx6 ade6-M216 leu1-32 ura4-D18	This study
YSM1798	h- ura4-294::nmt81:cdr2-GFP-tea4N-ura4+ pom1Δ::ura4+ tea4Δ::kanMX leu1-32	This study
YSM2177	pom1-cdr2-GFP-ura4+ tea4Δ::kanMX ade6-M216 leu1-32 ura4-D18	This study
YSM2178	pom1-cdr2C-GFP-ura4+ tea4Δ::kanMX ade6-M216 leu1-32 ura4-D18	This study
YSM2214	tea4Δ::kanMX pom1-mid1C-mCherry:leu+	This study
Fig. 4		
YSM2275	h+ ura4-294::nmt81:cdr2-GFP-Dis2-ura4+ tea4Δ::kanMX ade6- leu1-32	This study
YSM2276	ura4-294::nmt81:cdr2-GFP-Dis2-ura4+ tea4Δ::kanMX pom1- Tomato-NatMX ade6- leu1-32	This study
YSM2277	ura4-294::nmt81:cdr2-GFP-Dis2-ura4+ tea4Δ::kanMX pom1Δ::ura4+ ade6- leu1+	This study
YSM2278	h+ ura4-294::nmt81:cdr2-GFP-Dis2H247K tea4Δ::kanMX ade6? leu1-32	This study
YSM2279	ura4-294::nmt81:cdr2-GFP-Dis2H247K tea4Δ::kanMX pom1-Tomato-NatMX ade6? leu1-32	This study

YSM2333	ura4-294::nmt81:cdr2-GFP-Sds21-ura4+ tea4Δ::kanMX6 ade- leu1-32	This study
Fig. 5		
YSM2251	h+ ura4-294::nmt81:cdr2-GFP-tea4N-ura4+ tea4Δ::kanMX ade6-M216 leu1-32	This study
YSM2280	h- ura4-294::nmt81:cdr2-GFP-tea4N-ura4+ tea4Δ::kanMX tea1::ura4+ ade6-M216 leu1-32	This study
YSM2281	ura4-294::nmt81:cdr2-GFP-tea4N-ura4+ tea4Δ::kanMX exo70::nat ade6- leu1-32	This study
YSM2282	ura4-294::nmt81:cdr2-GFP-tea4N-ura4+ tea4Δ::kanMX for3::kanMX6 ade6- leu1-32	This study
YSM2283	h+ ura4-294::nmt81:cdr2-GFP-tea4N-ura4+ tea4Δ::kanMX rga4Δ::ura4+ ade6-M216 leu1-32	This study
YSM2284	h- ura4-294::nmt81:cdr2-GFP-tea4N-ura4+ tea4Δ::kanMX gef1::ura4+ ade6- leu1-32	This study
YSM2285	ura4-294::nmt81:cdr2-GFP-tea4N-ura4+ tea4Δ::kanMX rga4Δ::ura4+ gef1::ura4+ ade6- leu1-32	This study
YSM2267	h- ura4-294::nmt81:cdr2-mCherry-Tea4N-ura4+ tea4Δ::kanMX leu1-32::shk1 promoter:ScGIC2 CRIB:GFP3:leu1+ ade6-	This study
YSM2219	ura4-294::nmt81:cdr2-mCherry-Tea4N-ura4+ leu1-32::shk1 promoter:ScGIC2 CRIB:GFP3:leu1+-ura4+ tea4Δ::kanMX gef1::kanMX	This study
YSM2220	ura4-294::nmt81:cdr2-mCherry-Tea4N-ura4+ leu1-32::shk1 promoter:ScGIC2 CRIB:GFP3:leu1+-ura4+ tea4Δ::kanMX rga4Δ::kanMX	This study
YSM2301	ura4-294::nmt81:cdr2-GFP-ura4+ tea4Δ::kanMX gef1-tdTomato-NatMX	This study
YSM2302	ura4-294::nmt81:cdr2-GFPdis2-ura4+ tea4Δ::kanMX gef1-tdTomato-NatMX	This study
YSM2275	h+ ura4-294::nmt81:cdr2-GFP-Dis2-ura4+ tea4Δ::kanMX ade6- leu1-32	This study
YSM2246	ura4-294::nmt81:cdr2-GFP-Dis2-ura4+ tea4Δ::kanMX gef1::ura4+ ade6- leu1-32	This study
YSM2286	h+ rga4-GFP-KanMx6 leu1-32 ura4-D18	Tatebe et al, 2008
YSM2287	tea4^{SH3*}-HA-TEV-ProteinA rga4-GFP-KanMX6 ade6- leu1-32 ura4-D18	This study
YSM2288	tea4-HA-TEV-ProteinA rga4-GFP-KanMX6 ade6- leu1-32 ura4-D18	This study
YSM2289	tea4-HA-TEV-ProteinA pom1Δ::ura4+ rga4-GFP-KanMX6 ade6-	This study
YSM2334	ura4-294::nmt81:cdr2-GFP-ura4+ tea4Δ::kanMX for3::kanMX6 ade6- leu1-32	This study
Fig. 6		
YSM2180	ura4-294::nmt81:ppc89-GFP-tea4-ura4+ rga4-RFP-kanMX ade6+	This study
YSM2210	ura4-294::nmt81:ppc89-GFP-tea4-ura4+ rga4-RFP-kanMX pom1Δ::ura4+	This study
YSM2290	ura4-294::nmt81:cdr2-mCherry-Tea4N-ura4+ tea4Δ::kanMX rga4-GFP-KanMX6 ade6- leu1-32	This study
YSM2291	h+ ura4-294::nmt81:cdr2-mCherry-Tea4N-ura4+ leu1-32::nmt41:blt1-cytoRga4-GFP-leu1+ tea4Δ::kanMX rga4::KanMX ade6?	This study
YSM2292	h- ura4-294::nmt81:cdr2-mCherry-Tea4N-ura4+ leu1-32::nmt41:cytoRga4-GFP-leu1+ tea4Δ::kanMX rga4::KanMX ade6?	This study
YSM2293	ura4-294::nmt81:cdr2-mCherry-Tea4N-ura4+ leu1- 32::nmt41:cytoRga4-GFP-leu1+ tea4Δ::kanMX ade6?	This study
YSM2294	h- ura4-294::nmt81:cdr2-mCherry-Tea4N-ura4+ leu1- 32::nmt41:blt1-cytoRga4-GFP-leu1+ tea4Δ::kanMX ade6?	This study
YSM2275	h+ ura4-294::nmt81:cdr2-GFP-Dis2-ura4+ tea4Δ::kanMX ade6- leu1-32	This study
YSM2295	ura4-294::nmt81:cdr2-GFP-Dis2-ura4+ tea4Δ::kanMX rga4Δ::ura4+ ade6- leu1-32	This study
YSM2243	leu1-32::nmt41:blt1-cytoRga4-GFP-leu1+ ura4-294::nmt81:cdr2-GFP-Dis2-ura4+ tea4Δ::kanMX	This study
Fig. S1		
YSM2251	h+ ura4-294::nmt81:cdr2-GFP-tea4N-ura4+ tea4Δ::kanMX ade6-M216 leu1-32	This study
Fig. S2		
YSM2335	gef1-tdTomato-natMX CRIB-GFP-ura4+ sid4-mRFP-ura4+ ade6? leu1-32 ura4-D18	This study

Supplementary Table 2: Quantification of polarity factor localization

All quantifications were performed on single medial confocal planes, omitting cells in cytokinesis. In all cases, presence of signal at the lateral cell cortex was used was classified as positive. Where indicated, the presence of multiple signals was required to be classified as positive. Note that Dis2 side-signal was weak and difficult to distinguish from the normal cytosolic and actin patch localizations of Dis2.

Protein	**Notes**	**Cdr2-tea4N bulged cells**	**Cdr2-teaN non-bulged cells**	**Cdr2 cells**
Pom1-GFP		100% (122/122)	10% (104/104)	5% (5/93)
Tea1-GFP	at least two cortical dots in middle third portion	77% (36/47)	33% (17/51)	30% (17/57)
Scd1-3GFP		23% (20/87)	2% (1/54)	5% (3/61)
For3-3GFP	strong dots or patches	48% (35/73)	39% (49/126)	7% (12/176)
Myo52-tdTomato	at least three strong dots at lateral cortex	93% (68/73)	73% (76/104)	25% (21/84)
Exo70-GFP		67% (49/73)	52% (47/89)	13% (16/127)
Gef1-GFP		43% (168/388)	23% (123/531)	2% (7/335)
GFP-Dis2	at least two dots at lateral cortex	42% (44/106)	36% (53/147)	24% (74/310)
CRIB-GFP		76% (126/165)	44% (156/351)	7% (15/223)
CRIB-GFP rga4Δ		88% (7/8)	34% (82/241)	-
CRIB-GFP gef1Δ		- (1/1)	0% (0/204)	-

Table S3: Tea4-interacting proteins identified by Tea4-TAP

Numbers indicate the number of assigned spectra. Only proteins identified by 3 or more spectra in two independent purifications are shown. Rga4 is not indicated here, as it was identified only in one of the two experiments. We also did not identify Pom1 or For3 peptides in these experiments.

		Cultures grown in EMM			Cultures grown in YE			
Accession numbers	**Protein molecular weight**	**WT**	**Tea4-SH3*-TAP**	**Tea4-TAP**	**WT**	**Tea4-SH3*-TAP**	**Tea4-TAP**	**class / name**
TEA1_SCHPO	**127423**	**0**	**607**	**809**	**0**	**536**	**179**	**Tea1**
TEA4_SCHPO	**89546**	**0**	**179**	**210**	**0**	**213**	**82**	**Tea4**
TEA3_SCHPO	**127741**	**0**	**252**	**210**	**0**	**50**	**19**	**Tea3**
PP12_SCHPO	**36813**	**0**	**0**	**9**	**0**	**0**	**10**	**PP1, Sds21**
TCPQ_SCHPO	59938	0	5	8	0	8	4	T-complex
PP11_SCHPO	**37620**	**0**	**0**	**12**	**0**	**0**	**3**	**PP1, Dis2**
RPN1_SCHPO	97985	0	5	12	0	13	1	26S proteasome
IDH1_SCHPO	38742	0	6	9	0	2	1	mitochondrion
PRS4_SCHPO	50044	0	0	4	0	7	1	26S proteasome
ATPB_SCHPO	56859	0	6	22	0	3	0	mitochondrion
PRS6B_SCHPO	43536	0	11	9	0	9	0	26S proteasome
TCPZ_SCHPO	58532	0	0	8	0	12	0	T-complex
MAS5_SCHPO	44804	0	3	7	0	12	0	mas5
PRS6A_SCHPO	48820	0	0	5	0	6	0	26S proteasome
TCPA_SCHPO	60030	0	1	5	0	3	0	T-complex
RPN8_SCHPO	35577	0	0	4	0	3	0	26S proteasome
RUVB2_SCHPO	51545	0	0	3	0	4	0	DNA helicase
TCPG_SCHPO	58464	0	0	3	0	3	0	T-complex
CARA_SCHPO	45644	0	3	0	0	5	0	biosynthetic enzyme